Battery-Supercapacitor Hybrid Storage Scheme for Long-Life Solar Powered Wireless Sensor Networks

MTP Report submitted to

Indian Institute of Technology Mandi

for the award of the degree

of

M. Tech

by

Vikrant

under the guidance of

Dr. Satvasheel Powar and Dr. Tushar Jain

SCHOOL OF ENGINEERING

INDIAN INSTITUTE OF TECHNOLOGY MANDI

JUNE 2017

Dedicated to
my mother
Smt. Daya Wanti
and
my father
Shri. Udey Vir Singh

CERTIFICATE OF APPROVAL

14/06/2017

Certified that the MTP Report entitled Battery-Supercapacitor hybrid storage scheme long-life solar powered wireless sensor networks submitted by Vikrant to Indian Institute of Technology Mandi, for the award of the degree of M. Tech has been accepted after examination held today.

CERTIFICATE

This is to certify that the MTP Report entitled “**Battery-Supercapacitor hybrid storage scheme for long-life solar powered wireless sensor network**”, submitted by **Vikrant** to Indian Institute of Technology Mandi, is a record of bona fide work under our supervision and is worthy of consideration for the award of the degree of M. Tech of the Institute.

Dr. Satvasheel Powar

Dr. Tushar Jain

Date:

DECLARATION by the student

I solemnly declare that the data used for the work, the work depicted in the MTP Report, and the written material contained in the MTP Report are not copied from others and that due permission has been taken from, and due credit has been given to, the sources whenever they are used.

Name & Signature of Student/s

Abstract

A wireless sensor network is a network consisting of spatially distributed autonomous devices using sensors to monitor physical or environmental conditions. These autonomous devices are called sensor nodes. This work deals with the design of wireless sensing networks sensor node. Wireless sensing network uses sensors to monitor the physical environment for which the sensor nodes capable of sensing, computing, and receiving/transmitting are deployed in measurement(monitoring) field. The area of application ranges from environmental monitoring to monitoring the patient's condition in hospitals, the application requires them to be energy autonomous. Conventionally, a battery is used to power these sensor nodes; constraints such as limited battery life and capacity degradation with time limits the life and computational power of the nodes as well as increases their operating costs s they require frequent battery replacement. As substantial effort has been spent on the energy efficient routing to enhance the life of the system, this study proposes a battery-supercapacitor hybrid storage for solar powered WSN node for increasing the cycle life of battery and computation power. The presented simulation results show that the proposed system increases the cycle life of the battery by decreasing the charge-discharge cycles and increases the computational power.

Acknowledgments

I express my sincere gratitude to my guide Dr. Satvasheel Powar and Dr. Tushar Jain for their constant help, encouragement, and inspiration throughout the project work. Without their invaluable guidance, this work would never have been a successful one. I would also like to thank all the faculty members of the Department for their valuable suggestions and helpful discussions. Last, but not the least, I would like to thank my dearest and closest friends and of course, parents who have been the backbone, advisors and constant source of motivation throughout the work.

Contents

Abbreviations

PV = Photovoltaics
V_{PV} = Panel Voltage
I_{PV} = Panel Current
D = Duty Cycle
V_{BUS} = Internal DC Bus Voltage
P_{IN} = Input Power
V_{SC} = Supercapacitor Voltage
$V_{BATT.}$ = Battery Voltage
$I_{AVG.}$ = Average Current
E_{SOLAR} = Incident Solar Energy
$E_{ELECTRICAL}$ = Electric Energy
G = Insolation
I_D = Diode Leakage Current
I_{SH} = Shunt Current
P_{solar} = Power from PV Panel

List of Figures

List of Tables

Chapter 1

Introduction

1.1 Wireless Sensor Network

Wireless Sensor Network (WSN) is the second largest network after internet in the world, and it stands first in the list of ten emerging technologies [1]. WSN consist of a large number of sensor nodes spatially distributed in measurement field for sensing, transmitting and receiving information for performing tasks such as habitat monitoring, military surveillance, Smart buildings, environment monitoring such as greenhouse, water quality monitoring. WSN's are used for collecting the data when measurement field is large or located in difficult geographical terrain where round the clock surveillance is not possible.

The tiny sensor nodes are responsible for detection and transmission of data to the control room, the application requires them to be energy autonomous for performing the task. Conventionally, these sensor nodes are battery powered which require frequent replacement as the battery can sustain limited charge-discharge cycles without considerable loss in capacity [4].

The problem of powering a large number of sensor nodes densely deployed in the measurement field is restricting the use of WSN'S as it increases their operating costs. The possible solution to the above problem is to use energy harvesting from the ambient environment to power these nodes [1], which can be vibration, solar, acoustic noise etc. performance of each energy source depends on the environment of the measurement field. For most of the applications, solar outperforms other energy sources [5]. But like all other sources, it is intermittent in nature, so it requires storage mechanism.

Batteries are a matured technology and offer very high energy density in terms of charge storage [6]. To extend the rechargeable battery life as far as possible and keep the 'high performance' of the battery efficient charge-discharge control is required [7]. But this control is very difficult to implement if the nature of energy source is a variant. With all its disadvantages of like energy density, high leakage charge [6] supercapacitor is no way near to replace the battery as the storage mechanism, but it can offer its advantage in terms of virtually unlimited charge and discharge cycles [6].

In this work battery-supercapacitor, hybrid storage scheme is tested for its performance related to the lifetime of the sensor node in terms of charge-discharge cycles of battery since the battery is the limiting factor as it can sustain a limited number of charge-discharge cycles [6]. A power manager is used for efficient routing of energy.

1.2 Sensor Node

A sensor node is responsible for sensing, processing and receiving of data associated with the application. It consists of a processor capable of wireless transmission to which various sensors are interfaced. The sensor node doesn't send raw data it uses its processing ability to carry out simple computations and transmit partially processed data, for performing these functions it is equipped with a power source.

MICA2 Mote is generally used as a sensor node [4]. It is a tiny microcomputer with a TinyOS (TOS) Distributed Software Operating System. It's updated version MICA2DOT Mote is a third-generation mote module used for enabling low-power, wireless, sensor networks. The MICA2DOT is similar to the MICA2, except for its quarter-sized (25mm) form factor and reduced input/output channels.

Following are the features that make the MICA2DOT better suited for commercial deployment [31]:

- 868/916MHz, 433MHz or 315MHz multi-channel transceiver with extended range
- TinyOS (TOS) Distributed Software Operating System v1.0 with improved networking stack and improved debugging features
- Support for wireless remote reprogramming ·Compatible with MICA2 (MPR400) Mote
- On-Board Temperature Sensor, Battery Monitor, and LED

As the primary focus of this work is on increasing the lifetime of sensor node rather than reducing its power requirement. Therefore, Arduino Uno is selected as the processor, the reason being the ease with which it can be programmed and interfaced with various sensors. With the help of transmitter/receiver module, Arduino is capable of wireless communication. The entire assembly of Arduino, receiver/transmitter module, and the sensors is named as the sensor node.

1.3 Motivation

Application of WSN requires sensor nodes to be energy autonomous and without the need of battery replacement and disposal. Batteries as energy source require frequent replacement which is both costly and inconvenient. To make each node energy autonomous energy harvesting from ambient environment is used to power the sensor node, but due to intermittent nature of solar energy, the storage buffer is essential for reliability. Two schemes are available for energy storage, batteries and electrochemical double layer capacitors (supercapacitors) [9]. Each have their own advantages and limitations, batteries have high energy density and low leakage current than supercapacitors. However, supercapacitors offer the advantage in terms of the lifetime and high-power density. But the properties like low specific energy and high leakage charge makes them unsuitable to be used as primary storage in energy harvesting circuits as it would make the system more bulky and inefficient. Supercapacitors can complement battery and act as secondary storage as they have high power density and long lifetime in terms of large no of charge/discharge cycles the features in which battery lags. Battery-Supercapacitor hybrid storage scheme offers an advantage in terms of increase lifetime [10] but suffers from low efficiency due to high auto consumption of supercapacitor converter. For achieving high energy efficiency, we need to cater these issues.

1.4 Thesis Objective

As the major constraint for WSN is related with the lifetime of the sensor node and limited computational capability [11], which depends on cycle life of the battery. This work proposes a hybrid storage scheme with a power management algorithm aiming to increase the cycle life of the battery and to decrease the auto consumption of the supercapacitor converter. In this scheme battery act as primary storage and supercapacitor as secondary storage which combines the advantages of the supercapacitors in terms of lifetime and high-power density and the lithium batteries for their high energy density and cost. To use the storage schemes to the above effect a suitable power manager is required which implements a power management algorithm to switch the power circuit to certain predefined modes which allow it to operate at maximum efficiency under the operating conditions.

The key contribution of this work is the use of supercapacitors high power density with a suitable power management algorithm to increase the computational power of the sensor node.

1.5 Thesis Outline

The rest of the thesis is organized as follows: In Section 2, we give a brief description of the important papers that we have studied or utilized as a part of our literature survey. In Section 3, we introduce our proposed system architecture. Section 4 shows the simulation results. Whereas, Section 5 contains the details about hardware implementation. In Section 6 is devoted to the hardware implementation of proposed architecture.

Chapter 2

Literature review

Self-sustainable WSN’s are on the verge of being used as a mature technology in many fields involving defense and civil purposes [12]. Conventionally, sensor nodes are battery powered which require frequent replacement. Since WSN's find an application area where the sensor node will be either difficult or costly to maintain after the deployment, so researchers have scratched their head a lot on the problem to find out the renewable energy source that can be used to power these sensor nodes to make them energy autonomous and increase their lifetime. The available energy sources in the ambient environment that can be used for energy harvesting are solar, piezoelectric, vibration, thermoelectric and acoustic noise. From Table 1, it is clear that solar energy outperforms the other sources in terms of power density and is therefore preferred in energy harvesting circuits [13].

Table 1.

Power densities of energy harvesting technologies

Harvesting technology	**Power density**
Solar Cells (outdoors at noon)	15 mW/cm^2
Piezoelectric (shoe inserts)	330 $\mu W/cm^3$
Vibrations (small microwave oven)	116 $\mu W/cm^3$
Thermoelectric (10 °C gradient)	40 $\mu W/cm^3$
Acoustic noise (100 dB)	960 nW/cm^3

For indoor applications

Typically, the light intensity under artificial luminous found in hospitals and offices is less than 10 W/m^2 as compared to 100-1000 W/m^2 under outdoor conditions. For these light intensities efficiency of solar cells is very low. For example, efficiency for monocrystalline solar cells lies in the range of 1-3% and for amorphous cells, the range of efficiency is 3-7% [2]. Despite the fact that solar cells have poor efficiencies under indoor irradiance these cells offer power densities of at least 0.5–1 mW/cm^2 under 1–5 W/m^2 light intensity conditions, which is much higher than its nearest competitor [4]. Also, Solar cells are a mature technology hence it is easy to arrange a compact, efficient and cheap photovoltaic module. Therefore, solar energy harvesting is used for powering the sensor nodes in WSN.

Raghunathan et al. [1,4] presented Heliomote3, a solar harvesting module for sensor nodes equipped with 2 NiMH batteries and a small photovoltaic panel. This work focuses on harvesting system design that is capable autonomous operation and can manage all the decisions related to energy harvesting, energy storage, and energy supply. The ability of the system to modulate its power consumption by selectively deactivating its sub-components also impact the overall power management architecture. To realize the full benefits of energy harvesting it uses harvesting aware performance scaling algorithms and network protocols.

Minami et al. [14] presented a battery-less sensor node that is based on solar energy harvesting and uses electric double layer capacitor as storage buffer. The system was designed as a specialized system for supporting a typical scenario of environmental monitoring applications. Since the amount of energy obtained from the solar cell is small, a sensor node must wait for a long period until the capacitor has accumulated sufficient energy to start sensing and initiating wireless.

communication. This behavior of sensor node affects the design of the communication mechanism. To address this problem a new communication mechanism is designed. Although the concept of the system was successfully proven, the performance of the system was less than expected.

Jiang et al. [15] presented the design and implementation of Prometheus-- a Telos-mote based solar powered sensor node using two-stage storage buffers Li-ion battery and supercapacitor. The supercapacitor is used as primary storage and battery as secondary storage, primary and secondary refers to the order in which storage are exhausted by the sensor node. Prometheus also include a feature in which it can vary its duty cycle based on available power.

Fabio Ongaro et al. [10] presented a power management architecture for photovoltaics based WSN utilizing Li-ion battery and supercapacitor for energy storage. The primary objective of this work was to increase the node lifetime for achieving this supercapacitor's ability to sustain a large number of charge-discharge cycle is exploited by using a power management algorithm. Charge-discharge cycles of Li-ion battery were plotted against the supercapacitor capacity and it was shown that charge-discharge cycles decrease with increasing capacity of the supercapacitor. While the proposed power management architecture and statistical design approach may have a broad application. But the circuit prototype suffers from major limitations such as the auto consumption of supercapacitor converter is higher than the average power demand of the sensor node.

Degradation Mechanisms in Li-ion Batteries [2]

In the category of rechargeable batteries lithium based batteries are most commonly used as they have the advantage in terms of specific energy and is therefore preferred in compact designs. For understanding the charging strategy to be used in power management for the effective performance of the battery, it is essential to have a knowledge about the capacity degradation mechanism of the same.

- The charging mode consists of two phases, constant current and constant voltage.
- The constant current phase is responsible for charging the battery to a level of 70 to 80 % and consumes 20 to 30 % of total charging time.
- The constant voltage phase consumes 70 to 80 % of total time and the accumulated charge is only 20 to 30 % of total capacity.
- The constant voltage phase contributes little towards the capacity but accelerates the capacity degradation.
- The constant current phase should be done at low current ratings, 0.5 C is recommended.
- The discharge rates should be kept at a low level because the life-cycle depend proportionally on the discharge rates.

Chapter 3

Proposed approach

3.1 Architecture of the Proposed Power Management Circuit [10]

Fig. 1.1 Block diagram of the Power Circuit for Sensor Node

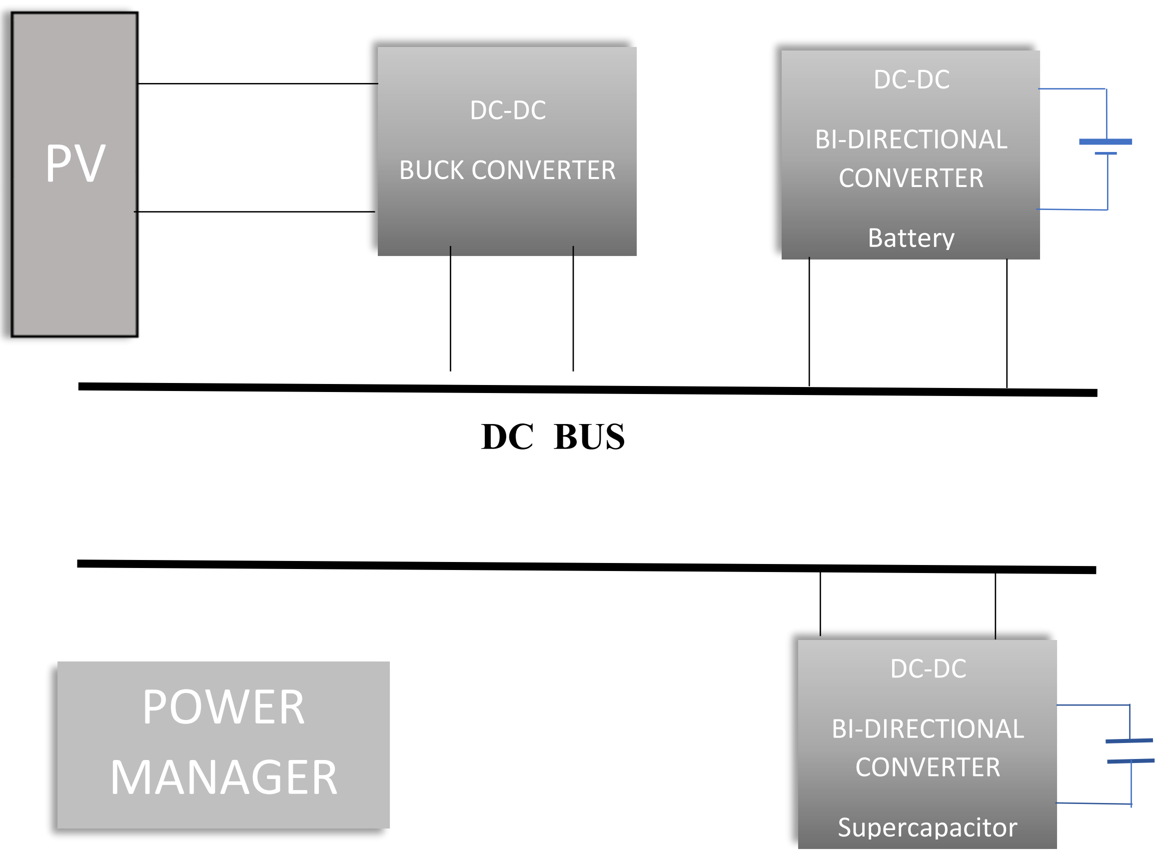

3.1.1 PV Module

It is used for solar energy harvesting which is the main source of energy for the sensor node. The output power from PV is not stable and depends on the irradiance and temperature. The output power from PV array is different at different irradiance and temperature level [17]. At the particular irradiance and temperature level, the P-V curve of the photovoltaic panel is non-linear and a maximum power point exists. Therefore, for maximum utilization of solar energy, we require a maximum power point tracker (MPPT). Detailed modeling of PV module and MPPT algorithm will be discussed in section 3.3.

3.1.2 Role of Battery and Supercapacitor

Li-ion battery and ELDC are used for electric storage. In which battery is used as primary storage and supercapacitor is used as secondary storage. This hybrid storage technique offers increased lifetime [10].

Due to low leakage charge battery is used for holding the charge for a long time and is discharged only when solar energy is not available and supercapacitor storage is exhausted.

The role of supercapacitor changes in accordance with the mode of operation, when solar power is available it smoothens the energy flow to match the charging profile of the battery and keep the voltage of the DC bus constant. During unavailability of solar power, the supercapacitor is dripped charged from the battery to supply the peak power. To check the inefficiency caused due to leakage charge supercapacitor is charged just before the arrival of the peak demand.

3.1.2 Role of Different Converters

The converters are used to control the power flow through the circuit. Although a wide variety of converter topologies are available, only a dozen basic ones are used in practical power design. The different converter topologies used in the proposed circuit are explained below: -

DC-DC Buck Converter

A Buck converter steps down the DC voltage and is required wherever source voltage is higher than the load voltage. This converter interfaces the PV panel with internal DC bus and is used to realize the MPPT of the panel. The controller adjusts the duty cycle of the switch to control the input voltage V_{PV} for maximum power point. For effectively controlling the input voltage, equation (1) suggest that V_{BUS} is kept constant.

$$\frac{V_{BUS}}{V_{PV}} = \frac{D}{1-D} \tag{1}$$

Fig. 1.2 DC-DC Buck Converter connected to the First Stage

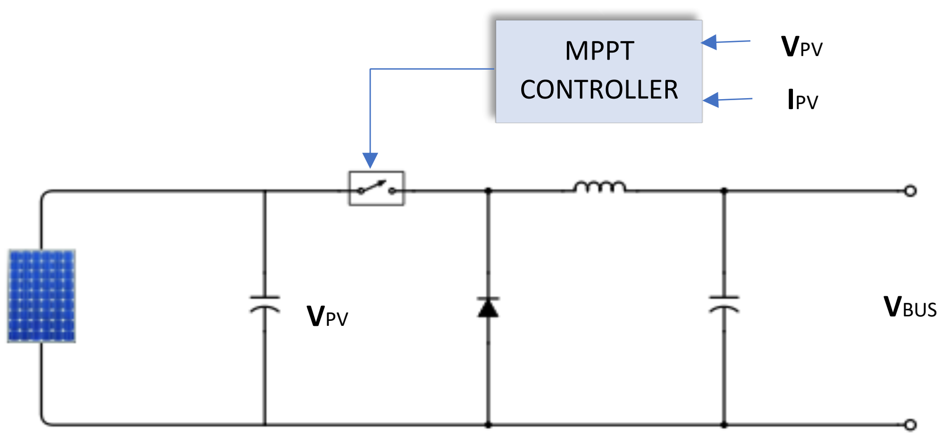

<u>DC-DC Buck Converter</u>

As the name suggest it is a bi-directional converter that is used to interface battery with DC bus. This converter allows bi-directional flow of power with different topologies. The converter operates in step-down mode during the charging process and in step-up mode while discharging. This choice is dictated by the voltage level of the battery with respect to the DC bus. The converter has a current controlled loop, reference for which is determined by the power manager.

Fig. 1.3 DC-DC Bi-directional Buck-Boost Converter connected to Battery

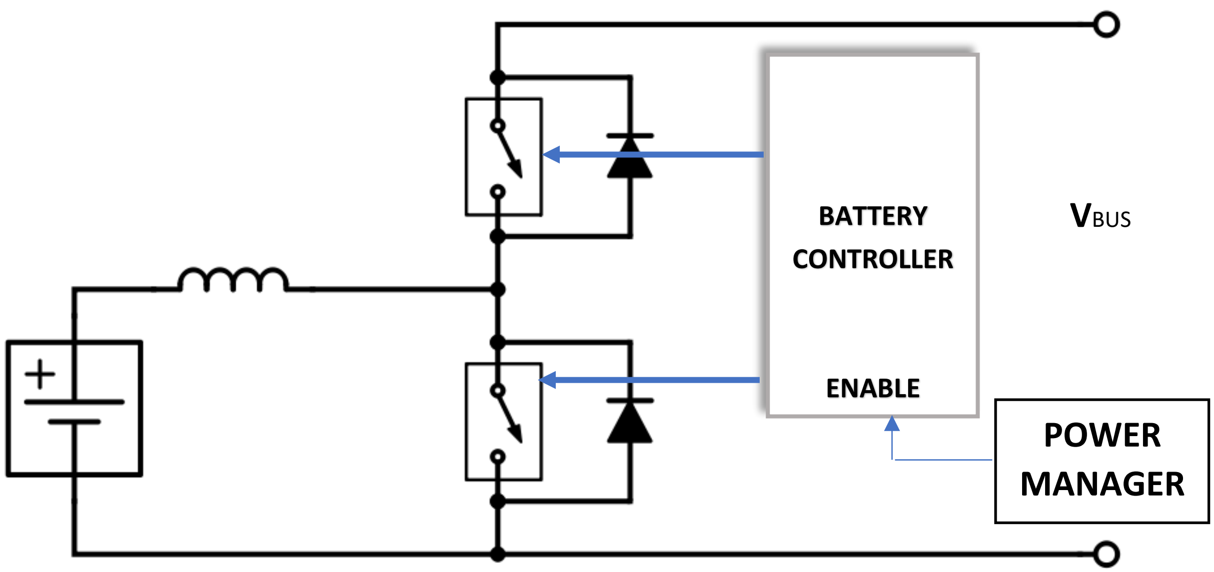

DC-DC Buck Converter

The dc-dc supercapacitor converter is a bidirectional converter, as shown in fig. 3.3. This converter is responsible for controlling DC bus voltage in a narrow band by acting as a source or sink depending on the instantaneous power budget. The proposed architecture is based on the direct transfer of solar power to load bus. Due to intermittent nature of solar energy, the energy mismatch between source and load is normal, which manifests as undesired conditions of under and over voltage on DC bus. Supercapacitor acts as a shock absorber to the system and smoothens out these energy fluctuations.

Fig. 1.4 DC-DC Bi-directional Converter connected to Supercapacitor

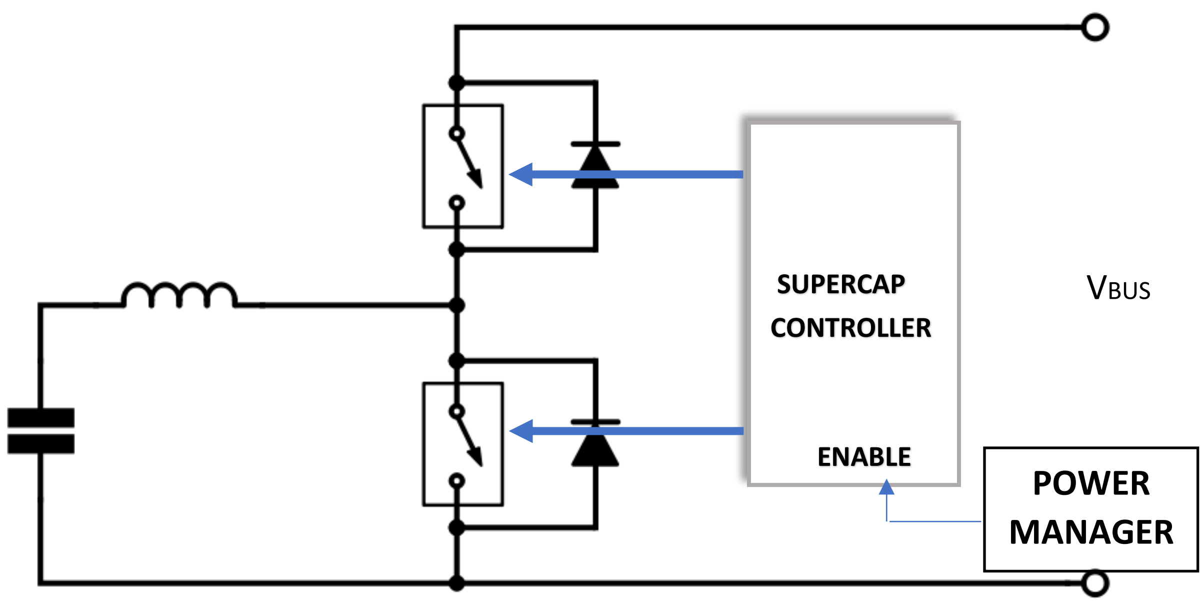

3.1.3 Power Manager

It is considered as the heart of the system as it is involved in all the decisions related to the control of the power circuit. Power manager helps in routing energy between supercapacitor, battery, and load to achieve high energy efficiency. To achieve this, it implements the power management algorithm which is basically based on some predefined states. The inputs to this block are input power (P_{IN}), supercapacitor voltage (V_{SC}) and battery voltage (V_{BATT}.). The detailed model of power management algorithm is presented in section 3.3.

Fig. 1.5 Power Manager Block Diagram

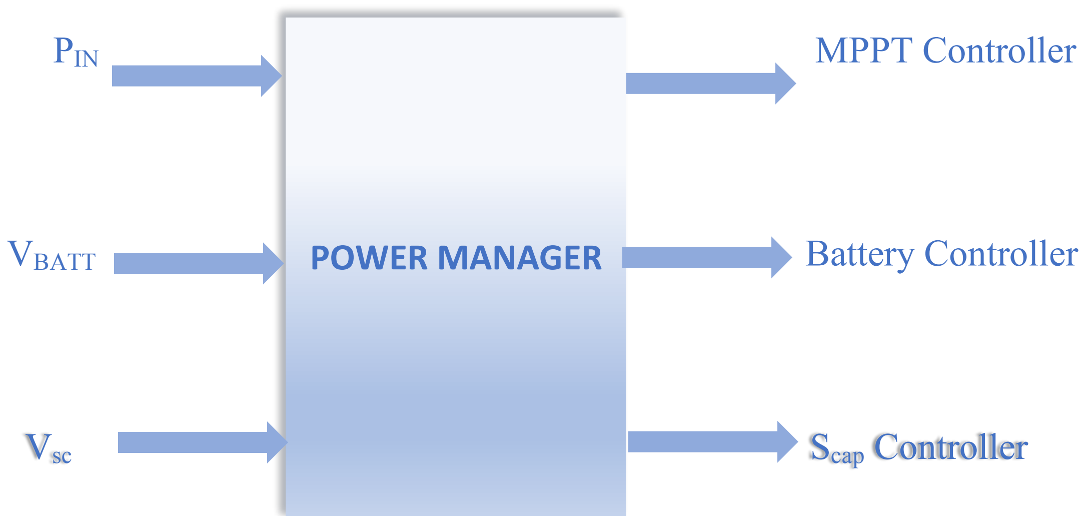

3.2 System Sizing

3.2.1 Power Consumption of the Sensor Node

Fig. 1.6 Cycle of Data Sensing

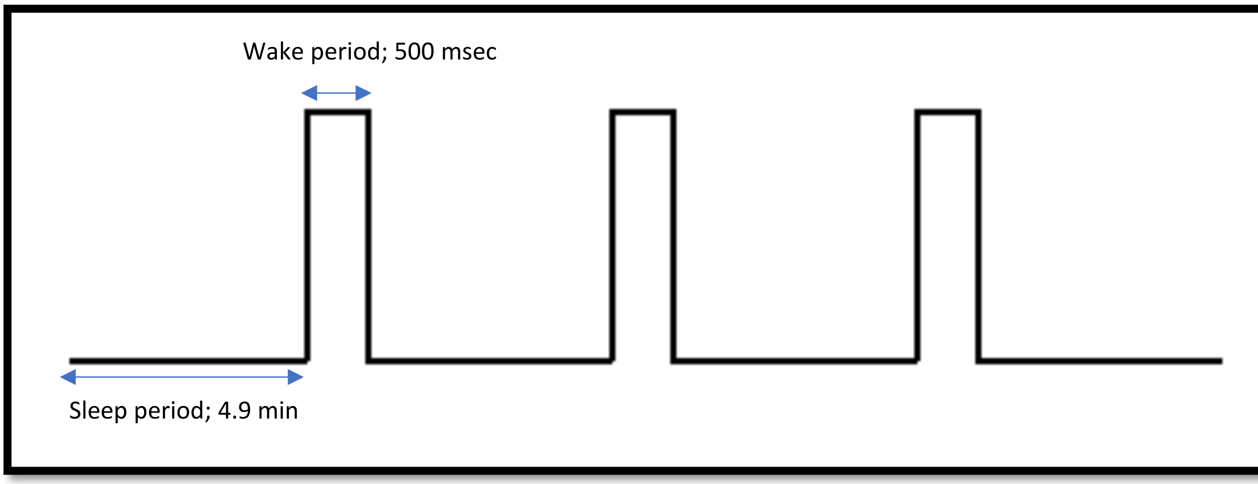

Figure 1.6 shows the current consumption profile for a WSN device with a 5 minutes wake cycle. For conserving energy WSN devices spend 99% of their lifetime in a low current sleeping mode which depends on the MCU used for the sensor node.

Arduino Uno is used as MCU for the reasons given in section 1 the parameters of which are given below: -

Active current = 100 µA

Sleep current = 50 mA

$$I_{AVG} = 0.1\times\frac{299.5}{300} + 50\times\frac{0.5}{300} = 0.183\text{ mA} \tag{2}$$

Over 24 hours period, the total current consumed will amount to 4.392 mAh

3.2.2 Storage Sizing

3.2.2.1 Battery Sizing [18]

Considering one week of autonomy, the minimum size of the battery is calculated as:

$$I_{AVG} \times 24 \times days\ of\ autonomy = 30.744 \text{ mAh} \quad (3)$$

One final consideration while sizing the battery is depth of discharge (DOD)

Fig. 1.7 Battery capacity degradation [2]

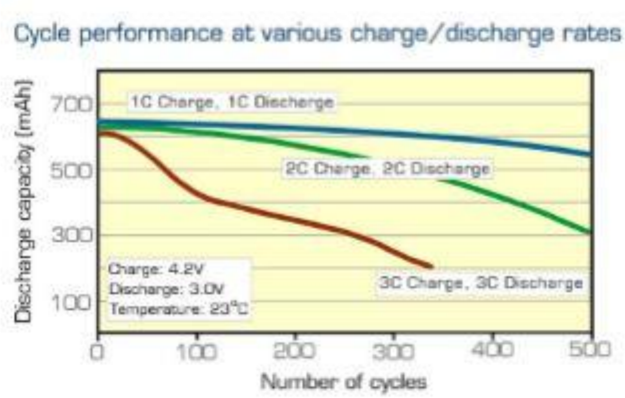

From figure 1.7, it can be concluded that for a given capacity, decreasing the charge and discharge rates by a factor of 2 will increase the lifetime of the battery by roughly the same amount. Therefore, the actual capacity of the battery will be higher than the minimum size required by the energy storage requirements.

For this work, a Li-ion battery of capacity 700 mAh is chosen for energy storage.

The charge/discharge depth is reduced to 30.744/700 (0.044C) and would result in a great increase in cycle life.

3.2.2.1 Supercapacitor Sizing

Supercapacitor has following two functions in the power circuit:

- It supplies the peak demand when power from solar is not available.
- It clamps the DC bus voltage to a constant value.

Minimum capacity of Supercapacitor required would be: - 50 F

$$\boldsymbol{C = \frac{2\times V_{load}\times I_{load}\times T_{peak}}{{V_{sc}}^{2}}}$$

This only decides the lower limit of the supercapacitor rating, for finding the actual storage size a detailed SIMULINK model is developed (Section 4) which is run for several hours and batteries charge/discharge cycles are plotted as the function of the capacity of the supercapacitor.

3.2.3 Solar Panel Sizing [18]

Insolation = 2.5 kWh/m^2

Total energy falling on an area of 1 m^2 over a period of one day will amount to:

$$E_{SOLAR} = 2500W\times 3600\,\frac{sec}{hour} = 9\ Megajoules \tag{4}$$

The equivalent electric energy generated will be:

$$E_{ELECTRICAL} = E_{SOLAR}\times Effective\_Area\times PV\_efficiency \tag{5}$$

Effective Area = 25mm by 100mm = 0.0025 m^2

PV efficiency = 3%

$E_{ELECTRICAL} = 9 \times 0.0025 \times 0.03 = 675\ Joules$ (6)

Capacity of the battery = 700 mAh

Battery voltage = 4.7 Volts

700 mAh of capacity at 4.7 Volts equates to a stored energy value of:

$700 \times 4.7 \times 3600 = 11844\ Joules$ (7)

Number of PV cells required = 11844/675 = 18 approximately (8)

3.2.4 Evaluation of Converter Parameters

Following are the parameters that are needed to be evaluated for all the converters introduced in section 3.1.2

- ✓ Inductor
- ✓ Input capacitor
- ✓ Output capacitor

For Buck Converter [19]

Inductor Selection

$$L = \frac{V_{OUT} \times (V_{IN} - V_{OUT})}{\Delta I_L \times f_s \times V_{IN}} \quad (9)$$

Where, V_{OUT} = desired output voltage

V_{IN} = typical input voltage

ΔI_L = estimated inductor ripple current

A good estimation for inductor ripple current is 20% to 40% of the output current

ΔI_L= (0.2 to 0.4)×$I_{OUT(max)}$

$I_{OUT(max)}$ = maximum output current

f_s = minimum switching frequency of the converter

Output Capacitor Selection

$$C_{OUT(min)} = \frac{\Delta I_L}{8 \times f_s \times \Delta V_{OUT}} \tag{10}$$

Where, ΔI_L= estimated inductor ripple current

ΔV_{OUT} = desired output voltage ripple

f_s = minimum switching frequency of the converter

The equivalent series resistance (ESR) of the capacitor adds some more ripple, given by:

$$V_{OUT(ESR)} = ESR \times \Delta I_L \tag{11}$$

Therefore, it is advised to use a low-ESR capacitor to minimize the ripple of the ripple on the output voltage. Ceramic capacitors are a good choice.

For Boost Converter [20]

<u>Inductor Selection</u>

$$L = \frac{V_{IN} \times (V_{OUT} - V_{IN})}{\Delta I_L \times f_s \times V_{OUT}} \tag{12}$$

Where, V_{OUT} = desired output voltage

V_{IN} = typical input voltage

ΔI_L= estimated inductor ripple current

A good estimation for inductor ripple current is 20% to 40% of the output current

ΔI_L= (0.2 to 0.4)×$I_{OUT(max)}$

$I_{OUT(max)}$ = maximum output current

f_s = minimum switching frequency of the converter

<u>Output Capacitor Selection</u>

$$C_{OUT(min)} = \frac{I_{OUT(MAX)} \times D}{f_s \times \Delta V_{OUT}} \tag{13}$$

Where, I_{OUT} = maximum output current of the application

ΔV_{OUT} = desired output voltage ripple

f_s = minimum switching frequency of the converter

D = duty cycle

$$D = \frac{I_L \times f_s \times L}{V_{IN(MIN)}} \tag{14}$$

Based on the equations (9-14) the value of parameters used for power circuit (fig. 1.8) are as follows:

Table

L_1	C_1	L_2	C_2	L_3	C_3
1 mH	$4.7\mu F$	100 mH	$26\mu F$	15 mH	$50\mu F$

Fig. 1.8 Equivalent Circuit of Power Circuit for the Sensor Node

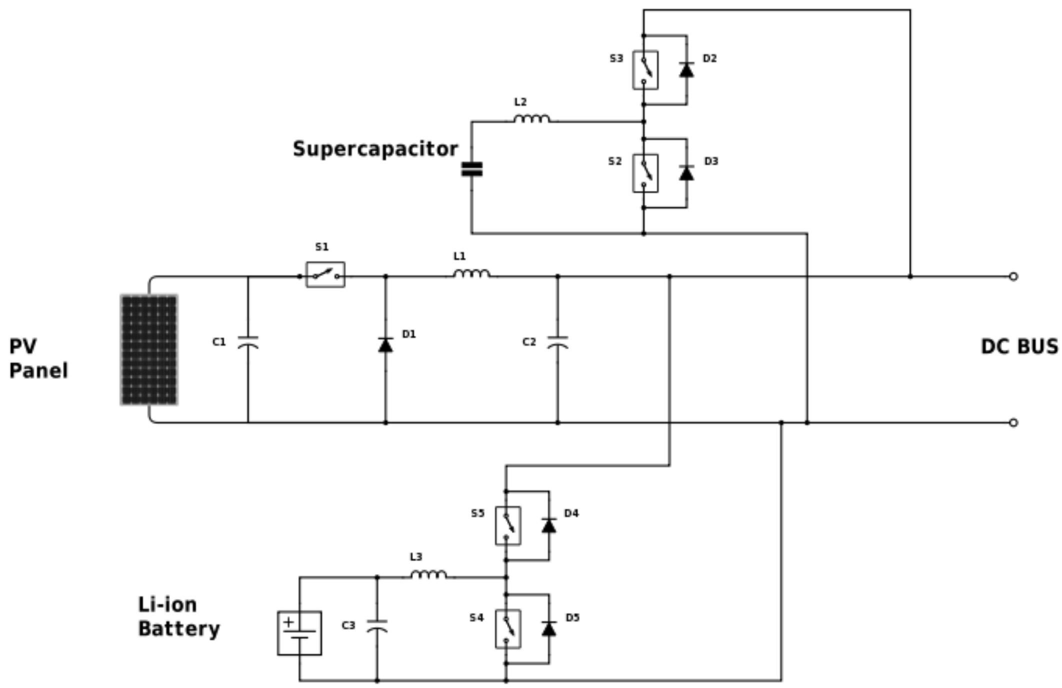

3.3 System Modelling

3.3.1 Solar Panel Modelling

The Physics of Photovoltaic cell

A solar cell is a solid electric device which consists of a p-n junction fabricated from a semiconductor material of moderate band-gap (usually silicon). It behaves as a normal p-n junction diode in dark and has non-linear V-I characteristics [21]. However, in the presence of light, it absorbs photons having energy greater than the band gap energy. This results in the creation of electron-hole pairs [22]. These charge carriers are separated by internal electric field and result in a current proportional to incident photons.

PV Cell Model

A simplest equivalent circuit of a solar cell is shown in fig. (3.9). It consists of a current source in parallel with a diode [8]. The output of the current source is proportional to the incident photon flux this current is called photocurrent. During darkness, the solar cell is not active and behave as an ordinary p-n junction diode and this gets modeled as a diode in the equivalent circuit [32]. It produces neither a current nor a voltage. This comes into action whenever a potential difference exists between the terminals of the solar cell and constitutes a current called Dark current. This diode determines the I-V characteristics of the solar cell [32].

Following are the parameters which are needed to be considered for accurate modeling of PV cell: -

- ✓ Temperature dependence of the diode saturation current (reverse) I_S.
- ✓ Temperature dependence of the photo current I_{ph}.
- ✓ Series resistance R1 [20], representing internal losses due to current flow.
- ✓ Shunt resistance R2 [20], in parallel with the diode, this corresponds to the leakage current.

Fig. 1.9 Equivalent Circuit of Solar Cell [23]

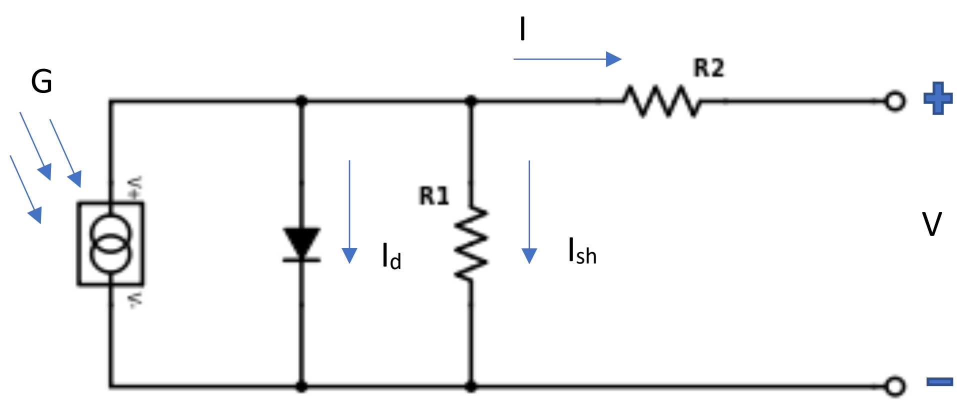

Equations which are used to model the PV cell in MATLAB Simulink [24], [25]:

$$1.\ V_t = \frac{kT_{op}}{q} \tag{15}$$

$$2.\ V_{oc} = V_t\, ln\left(\frac{I_{ph}}{I_s}\right) \tag{16}$$

$$3.\ I_d = \left[e^{\frac{(V+IR2)}{nV_tCN_s}} - 1\right] I_s N_p \tag{17}$$

4. $I_s = I_{rs}\left(\frac{T_{op}}{T_{ref}}\right)^3 e^{\left[\frac{qE_g}{nk}\left(\frac{1}{T_{op}}-\frac{1}{T_{ref}}\right)\right]}$ (18)

5. $I_{rs} = \frac{I_{sc}}{\left[e^{\left(\frac{V_{oc}q}{kCT_{op}n}\right)}-1\right]}$ (19)

6. $I_{sh} = \frac{V+IR2}{R1}$ (20)

7. $I_{ph} = G_k[I_{sc} + k_I(T_{op} - T_{ref})]$ (21)

8. $I = I_{ph}N_p - I_d - I_{sh}$ (22)

Detailed Simulink Model of PV Module based on above equations

Fig. 1.10 Equivalent circuit of PV Panel in Simulink

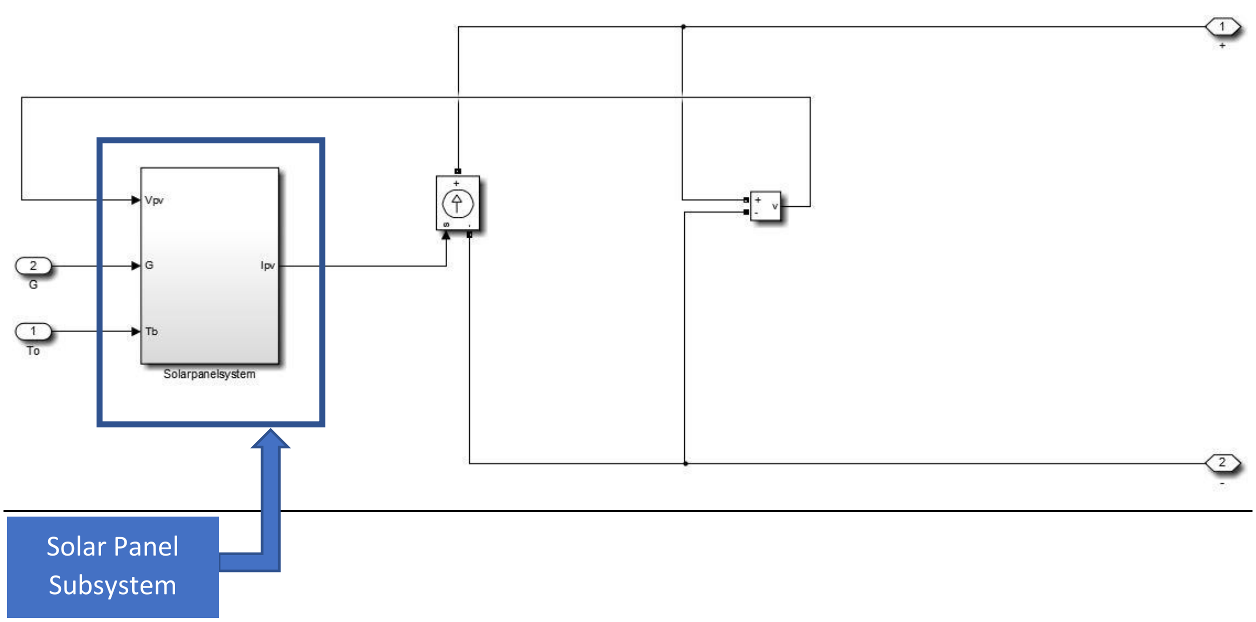

Fig. 1.11 Insite of Solar Panel Subsystem

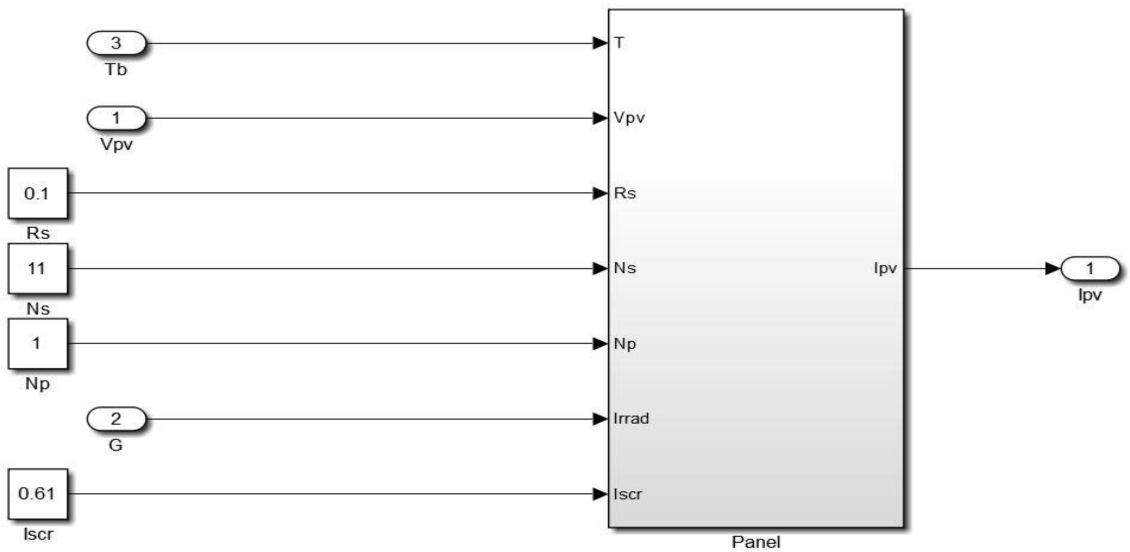

Fig. 1.12 Insite of Panel Subsystem

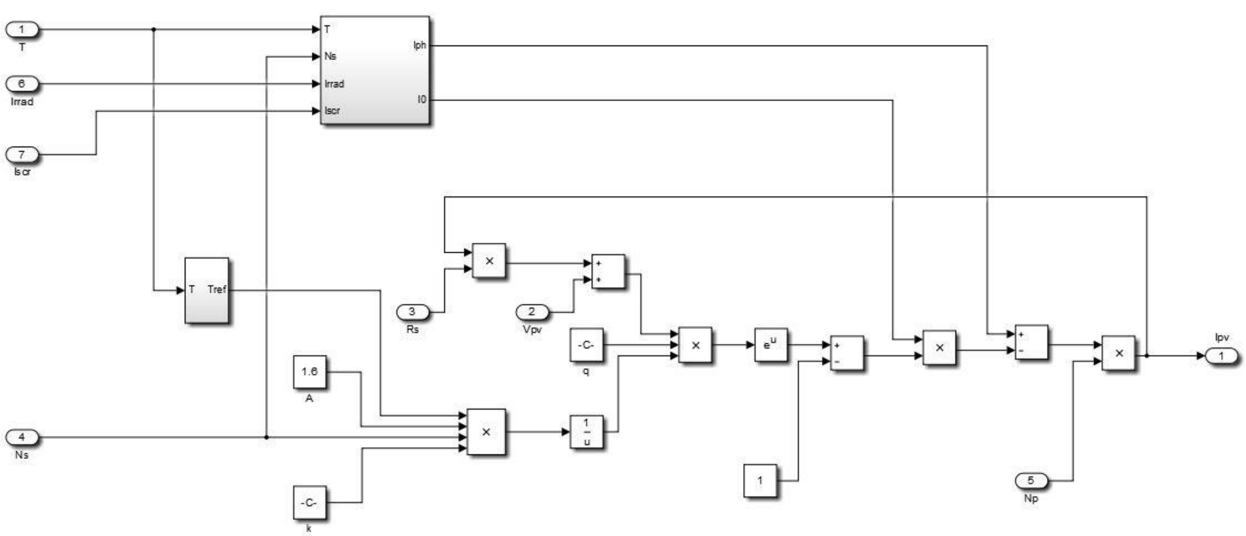

Fig. 1.13 Calculation of I_{ph} and I_o

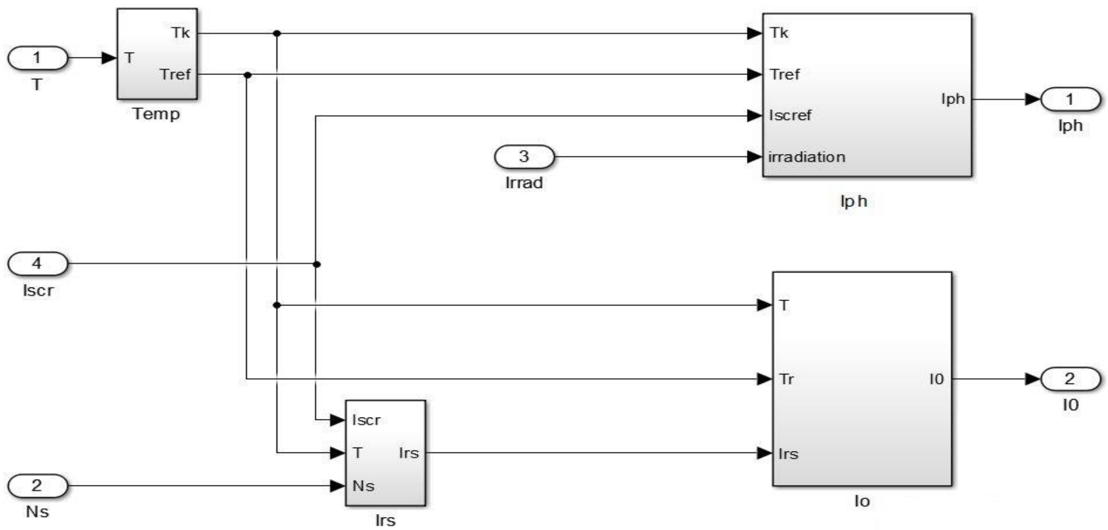

Fig. 1.14 Calculation of I_{ph}

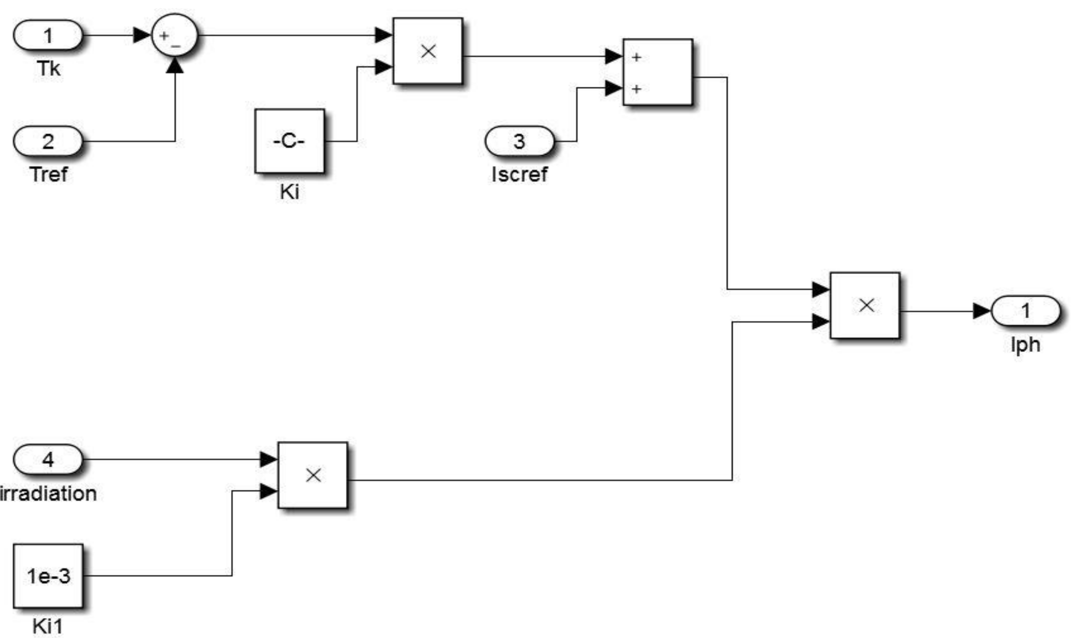

Fig. 1.15 Calculation of I_O

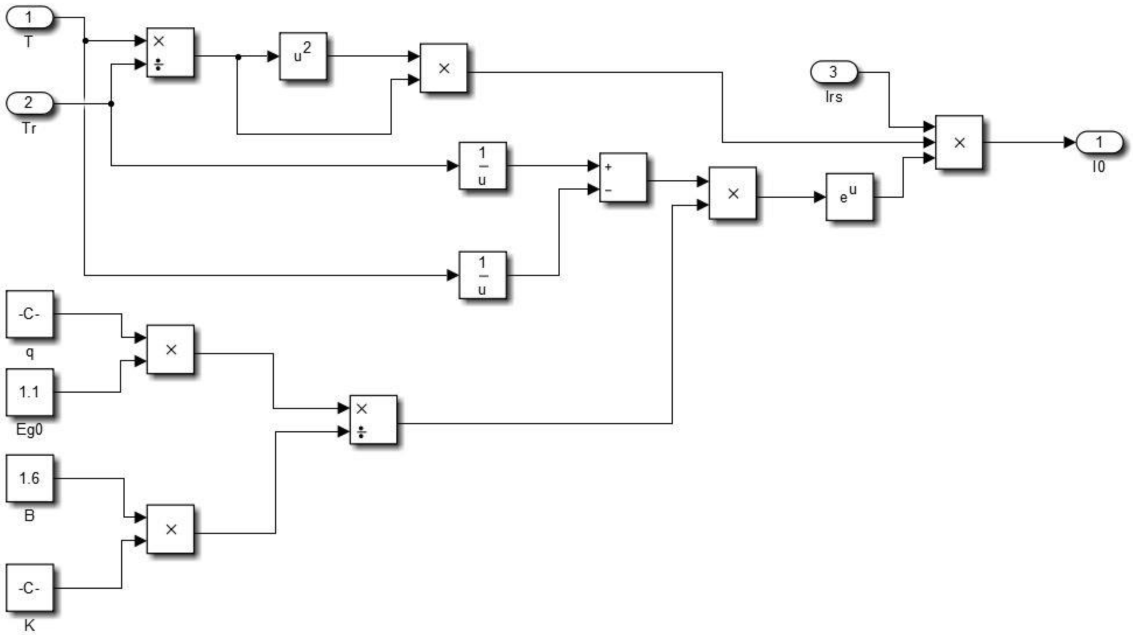

3.3.2 MPPT Algorithm

Solar panels have a non-linear P-V curve at a particular irradiance and temperature and maximum power point exists to track this we need MPPT algorithm. Several methods are present in literature to realize MPPT, each technique has one or more advantage over the other. Some of the most popular techniques are listed as:

- ✓ Perturb and Observe (P and O)
- ✓ Incremental Conductance (IC)
- ✓ Fractional Open Circuit Voltage (FOCV)
- ✓ Fractional Open Circuit Current (FOCI)
- ✓ Neural Network

Among these techniques most commonly used are "P and O" and "Incremental Conductance". In this work Perturb and Observation technique is used for tracking MPP. This is based on hill climbing technique and is easy to implement and gives a good performance when irradiation is constant.

Flowchart of Perturb and Observe algorithm [26]

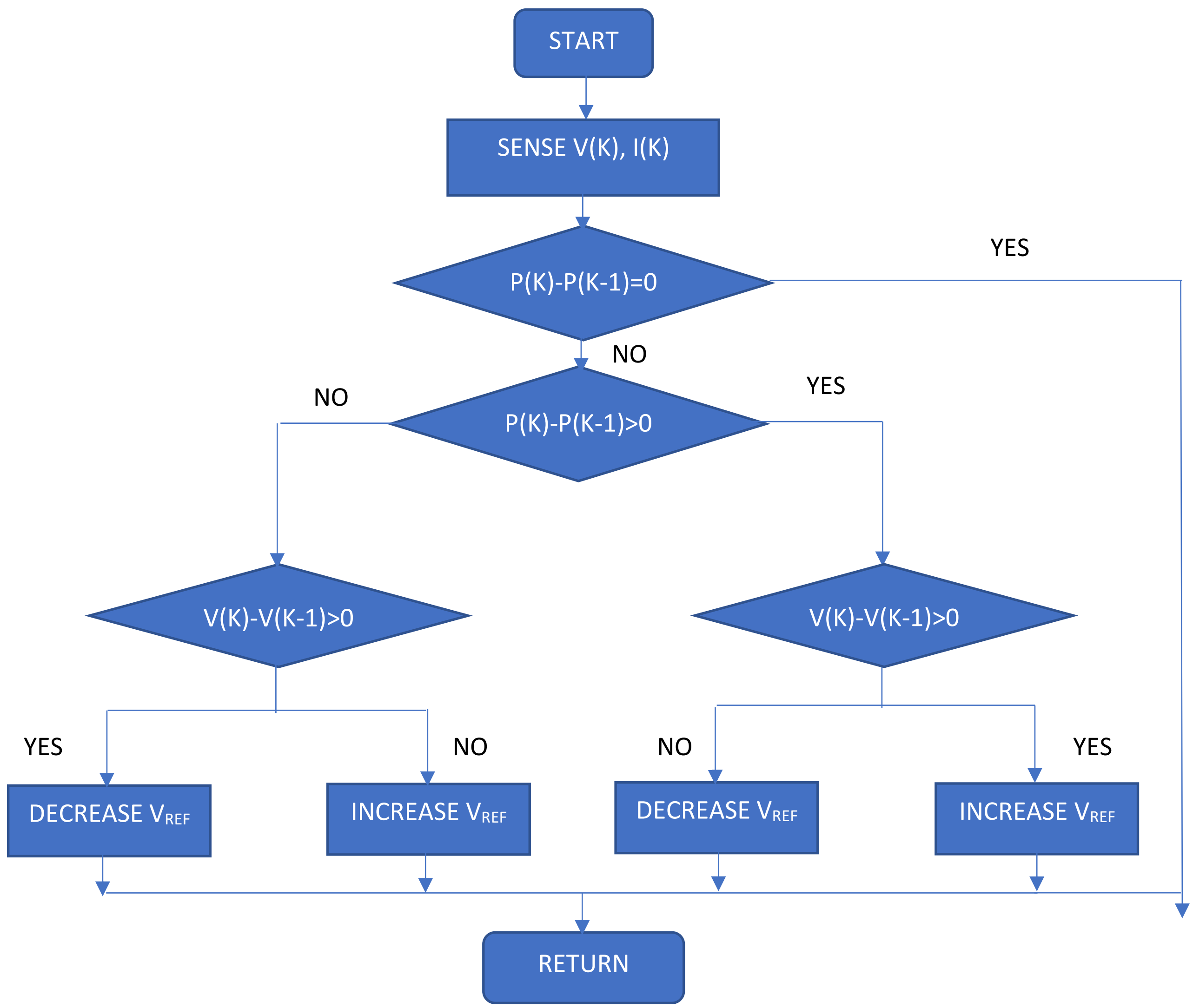

Fig. 1.16 SIMULINK Model of P and O Algorithm

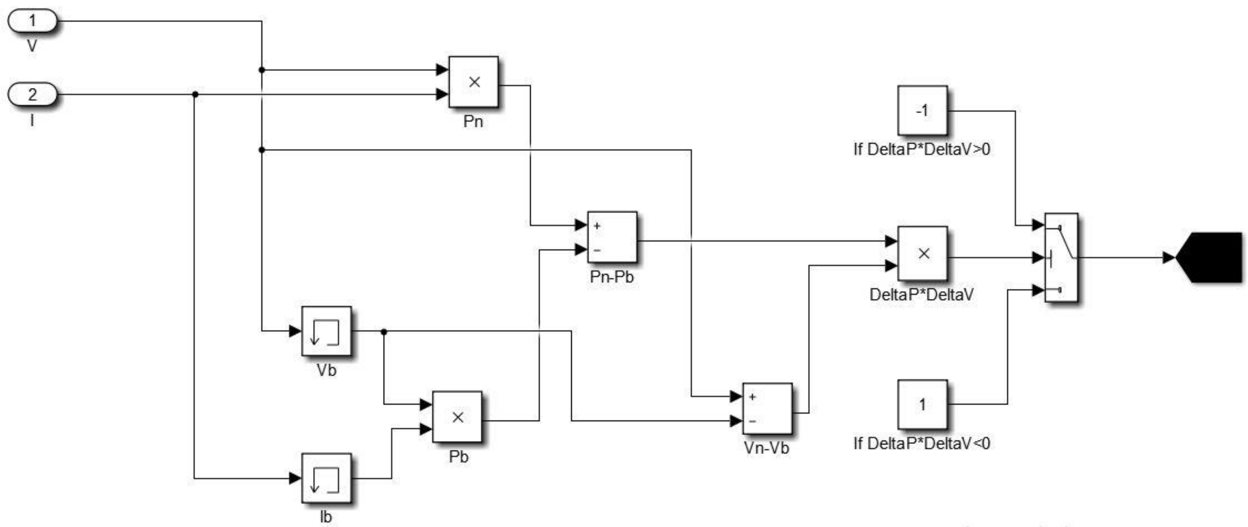

Fig. 1.17 Pulse Generation

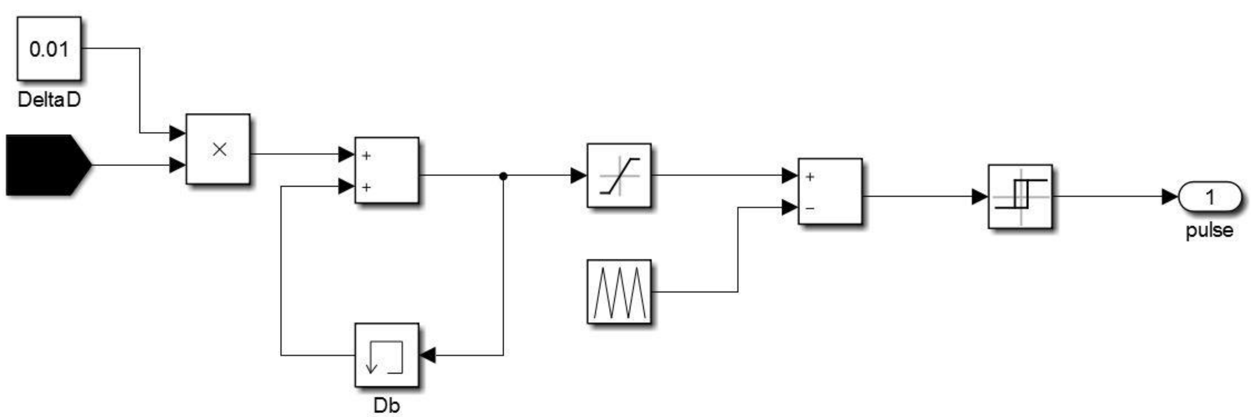

3.3.3 Power Management Algorithm

The role of the Power Manager in the proposed architecture has been discussed in section 2. This section contains the detailed Simulink model of power management algorithm which is based on six different states. These states are further divided into two groups depending on power from solar is available or not.

States of Power Management Algorithm when Solar Power (P_{SOLAR}) is available:

OFF State: - All the storages are discharged, all the converters are disabled

Soft Start: - P_{SOLAR} is greater than the power required by controller to turn on

Battery Charge: - This mode is enabled when V_{SC} reaches 1.9 Volts, this ensures that the system has enough energy to supply constant current for battery charging.

Overvoltage: - When V_{SC} reaches to a voltage greater than its maximum voltage limit this mode gets activated and requires MPPT to be disabled as P_{SOLAR} is greater than the load and battery charging requirement.

Disable Battery Charge: - When battery voltage reaches at floating value (4.2 Volts)

States of Power Management Algorithm when Solar Power (P_{SOLAR}) is not available:

Battery Charge Supercapacitor: - This mode is activated just before the arrival of peak load and depends on the duty of the data sensing. During this mode, supercapacitor is drip charged from the battery to a value sufficient enough to supply peak load.

Power manager switches the system from one mode to other by tracking battery voltage, input power, and supercapacitor voltage.

States of Power Management Algorithm when P_{solar} is available: -

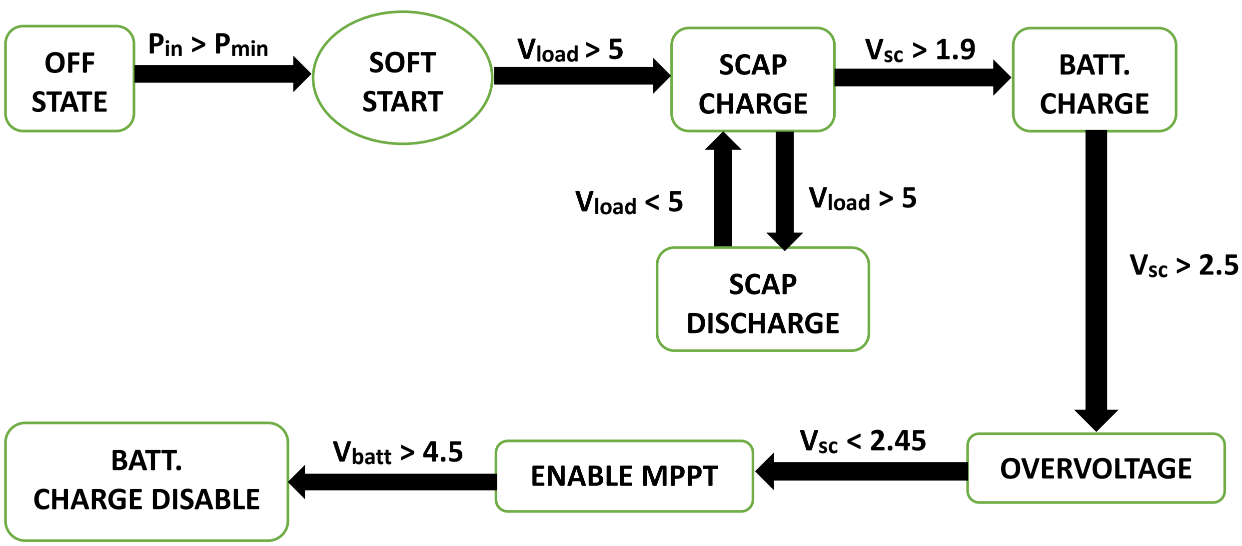

States of Power Management Algorithm when P_{solar} is not available: -

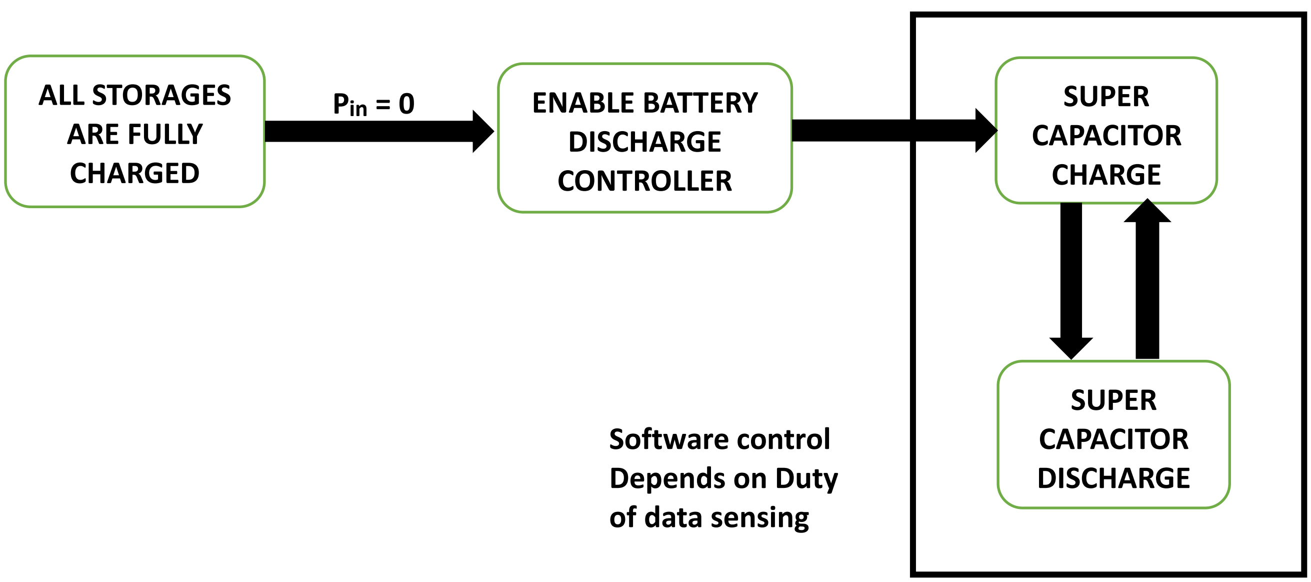

Simulink Model of Power Manager: -

Fig. 1.18 MPPT Controller Enable/Disable Control

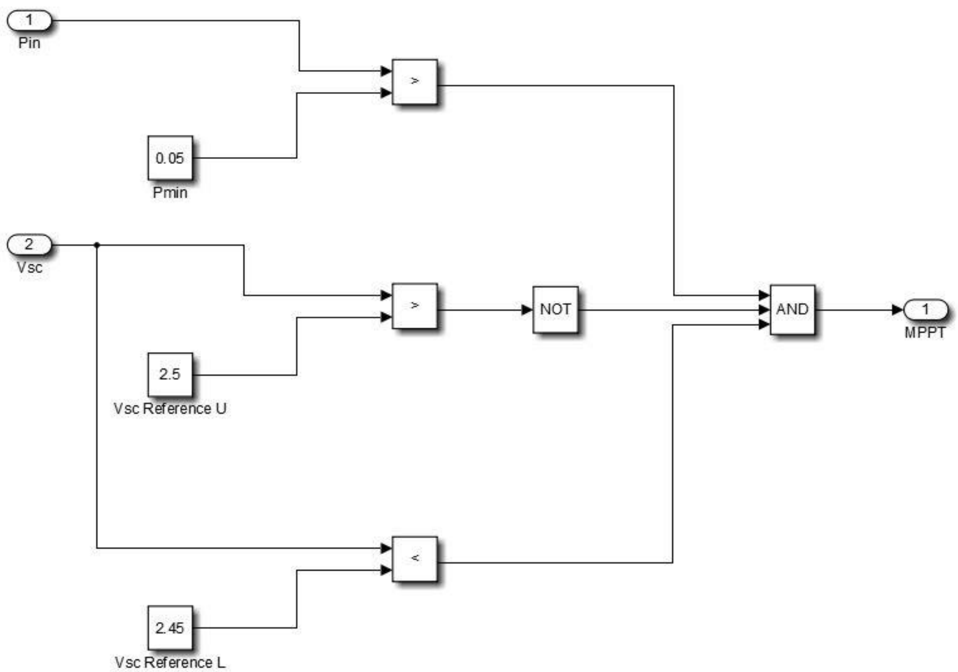

Fig. 1.19 Battery Discharge Controller Enable/disable Control

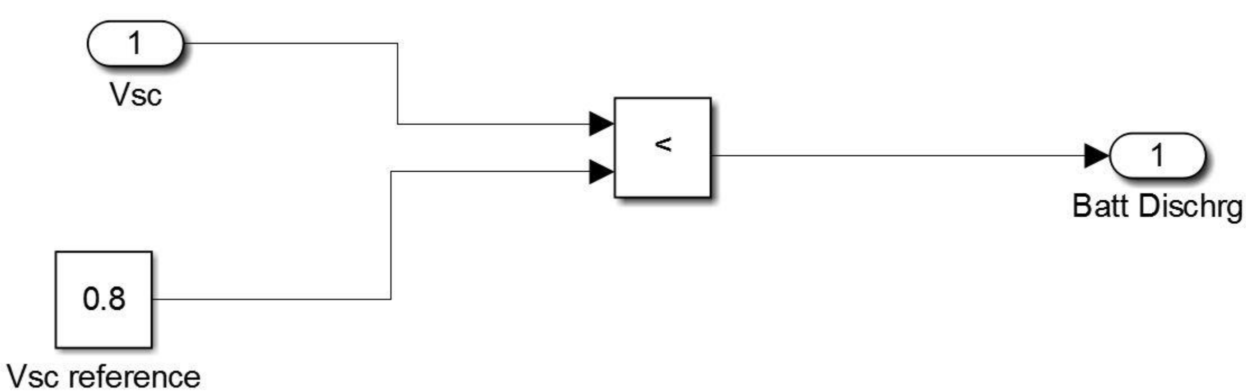

Fig. 1.20 Battery Charge Enable/Disable Control

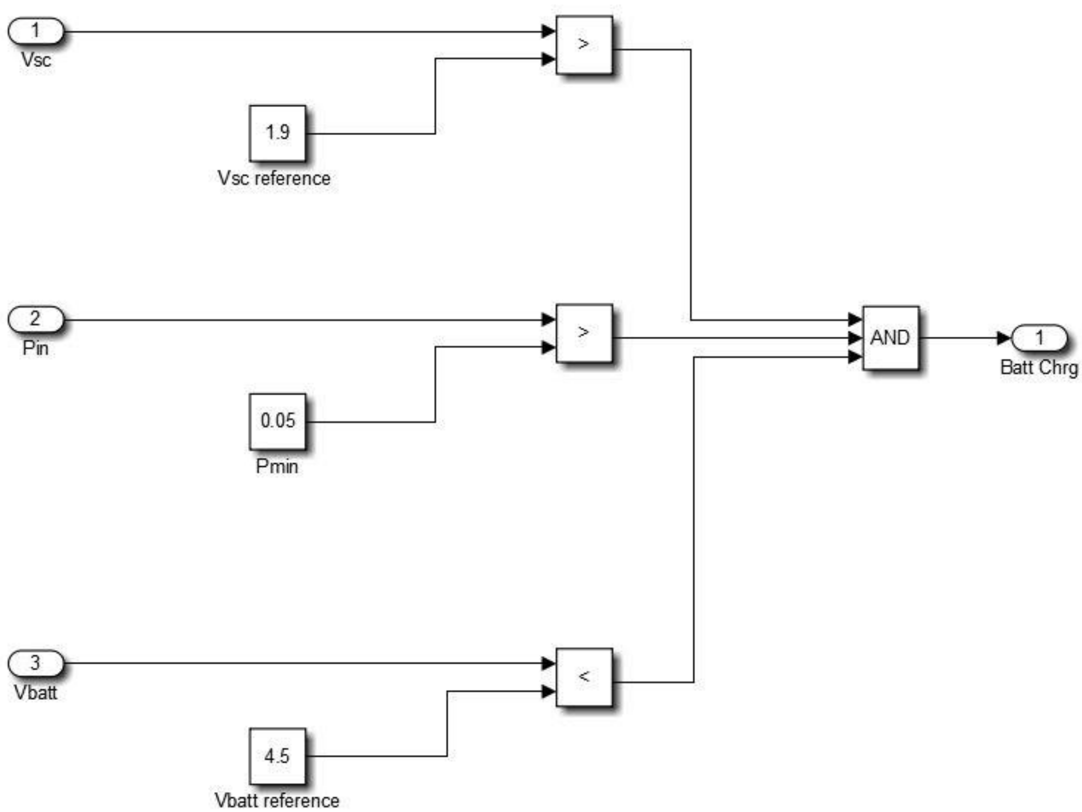

Fig. 1.21 Battery Charge Supercapacitor Controller Enable/Disable

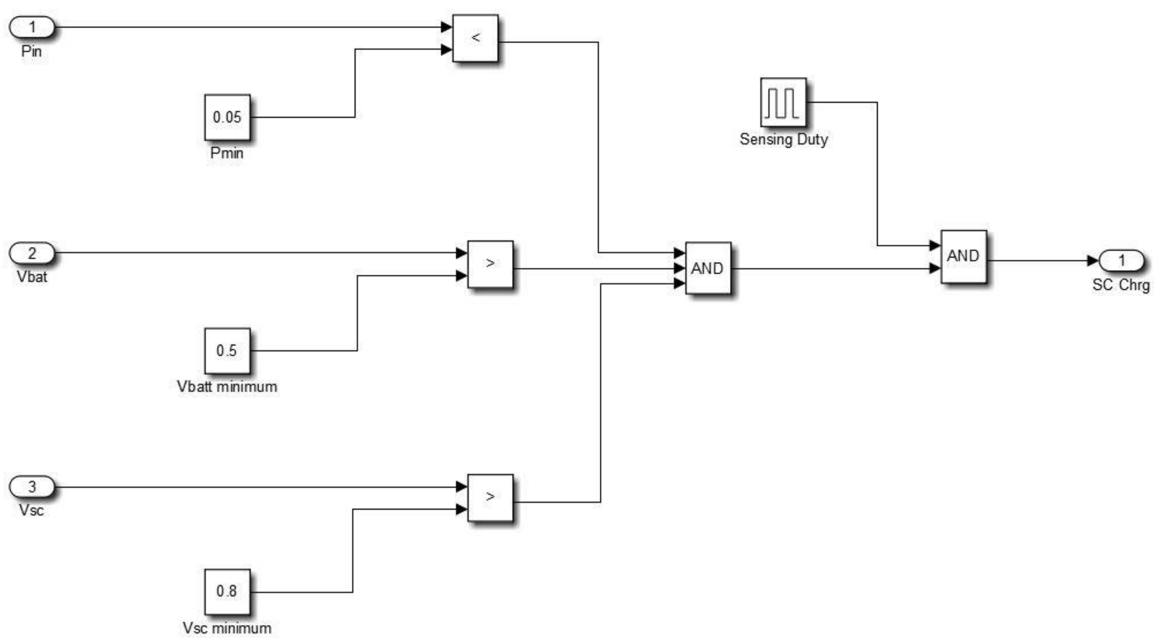

3.3.4 Controllers

3.3.4.1 Battery Charge-Discharge Controller

Charge Controller

For avoiding capacity degradation constant voltage charging mode [10] is not used so the charge controller has to control the charge current only, a variable duty cycle generator based on hysteresis control is used as the charge controller.

Discharge Controller

Two types of discharge controllers are used one for providing the load current to the system and second (Battery charge Scap Controller) for charging supercapacitor when P_{SOLAR} is not available. The need for this controller arrives due to very small impedances of battery and supercapacitor, direct charging will result in a very high current (about 500 Ampere's) which will destroy the battery.

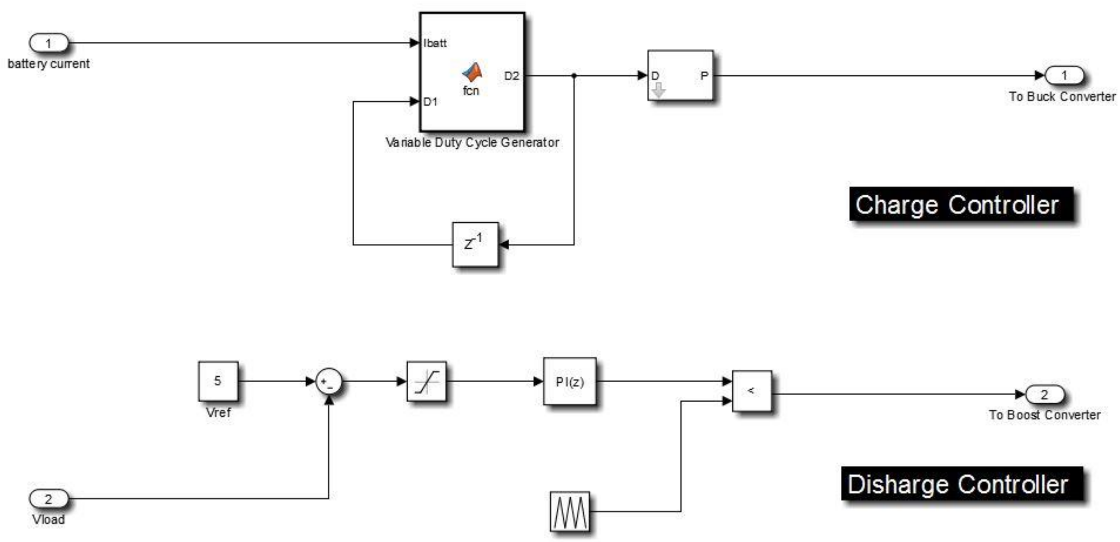

Variable Duty-Cycle Generator

MATLAB Program

```
function D2 = fcn(IBATT, D1)
%# codegen
D = D1;
D = 0.09;
if (IBATT >= 0.750)
D = D – 0.005;
elseif (IBATT < .700)
D = D – 0.0003;
end
end
```

Battery Charge Scap Controller is same as Variable Duty-Cycle generator except that the current limits are as follows: -

Upper limit = 0.350 Ampere's

Lower limit = 0.300 Ampere's

3.3.4.2 Supercapacitor Charge-Discharge Controller

A single double loop PI controller is used for implementing charge-discharge controller, the outer loop is slow acting and act as master and decides the reference for inner loop which is fast in action and acts as slave to the outer loop.

Fig. 1.23 Supercapacitor Charge-Discharge Controller

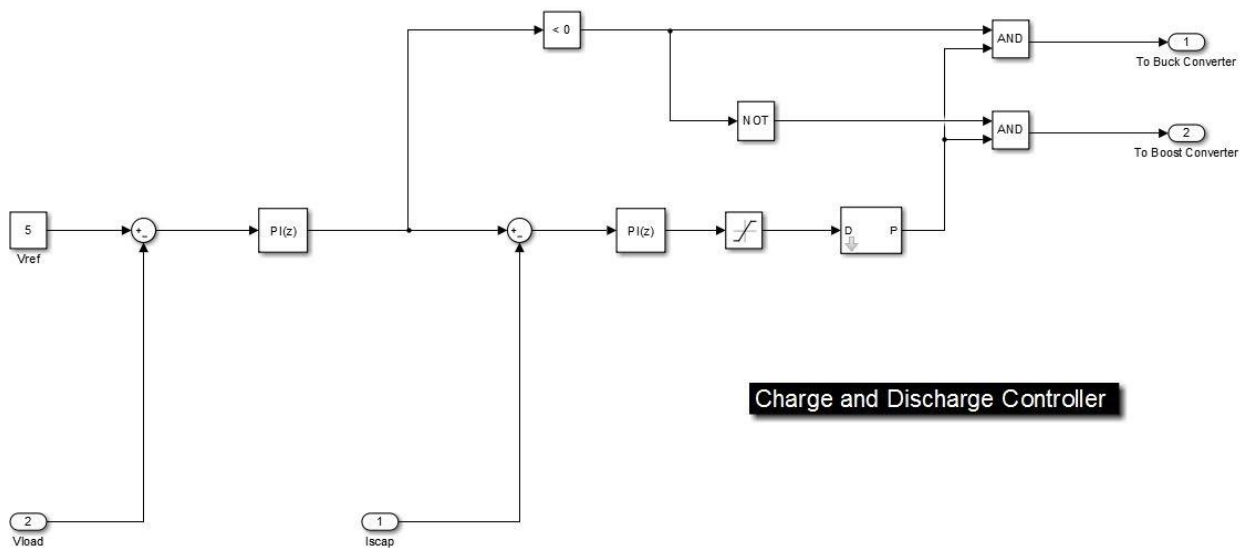

Chapter 4

Simulation Results

Fig. 1.24 P-V Characteristics of the Panel

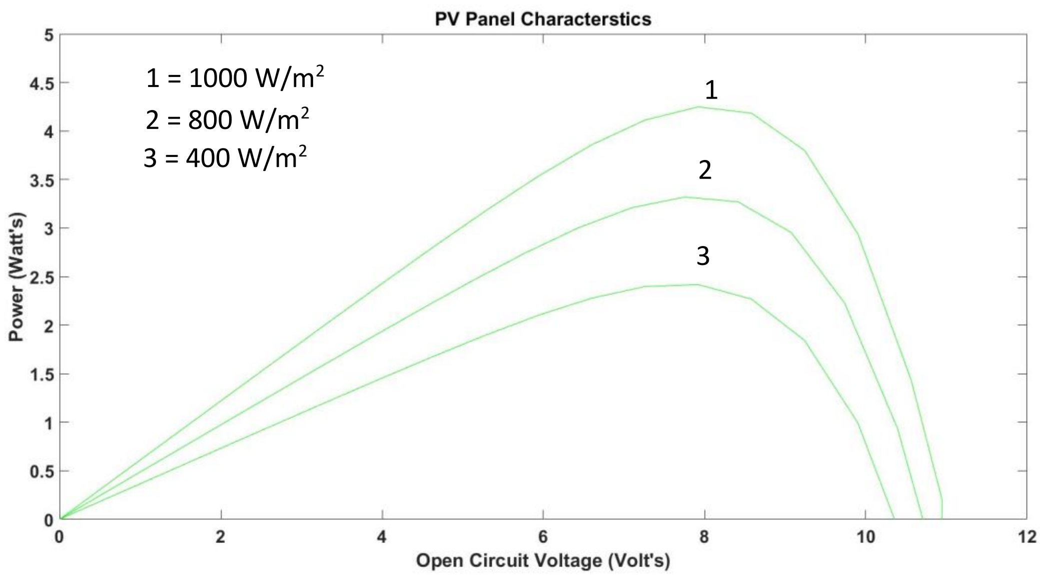

Fig.1.24 Shows the plot of P-V characteristics of the PV Panel under different values of Illumination marked as 1,2, and 3 (@ 25°C), which are in coherence with the non-linear characteristics of the panel . The detailed model is present in section 3.3 and following are the values of the different parameters used in modeling: -

I_{mp}	V_{mp}	$P_{max,e}$	K_v	K_i	α	R_1	R_2	I_{pv}
0.61 Amperes	6.5 Volts	4.5 Watts	-0.123 V/K	0.0032 A/K	1.3	415.405 Ohms	0.1 Ohms	0.73 Amperes

Performance of the MPPT and Battery Charge/Discharge Controller

Fig. 1.25 PV Charging Battery

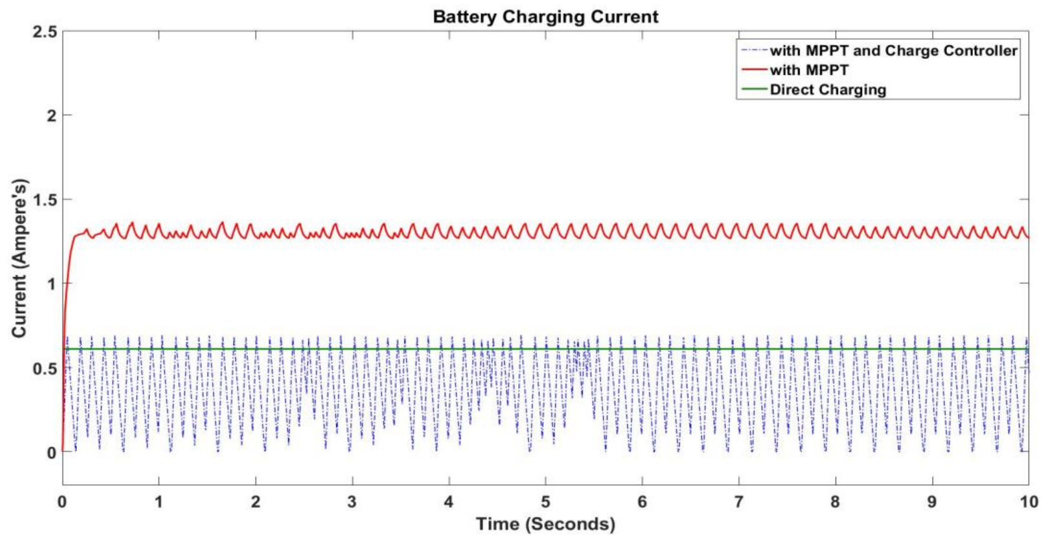

From figure 1.25, it is clear that MPPT Controller is boosting battery charging current from 0.5 Amperes (Green color) to 1.2 Amperes (Red Color) and with the controller it is regulated to 0.55 Amperes (Blue Color), with charge controller the charge rate is reduced which in turn will help in increasing the cycle life of the battery [10].

Fig. 1.26 PV Power while Charging Battery

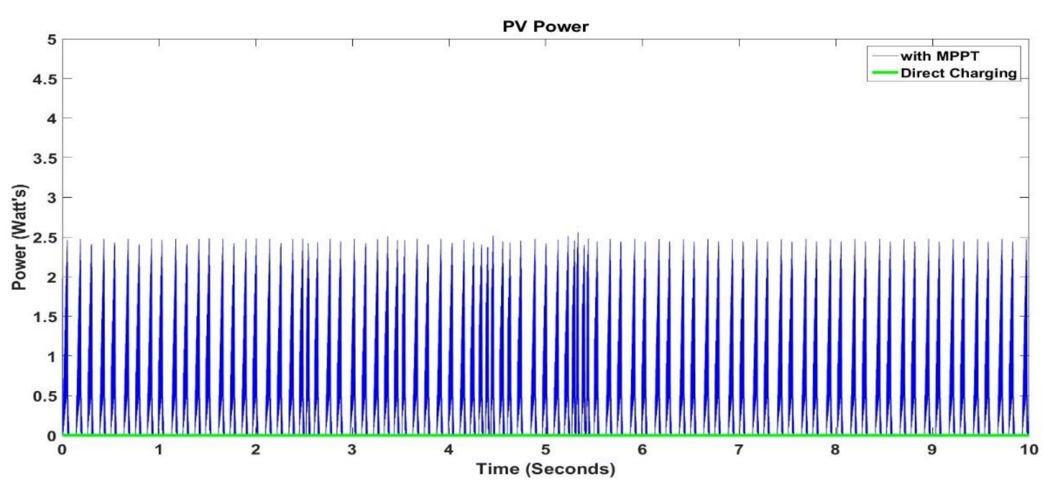

Fig 1.26 compares the battery charging power with (blue) and without the (green) charge controller. It clearly shows that with the controller the PV is able to operate at MPP. This power corresponds to MPP and is panel peak power at irradiance 500 W/m^2 and temperature 25 °C.

Fig. 1.27 PV Voltage while Charging Battery

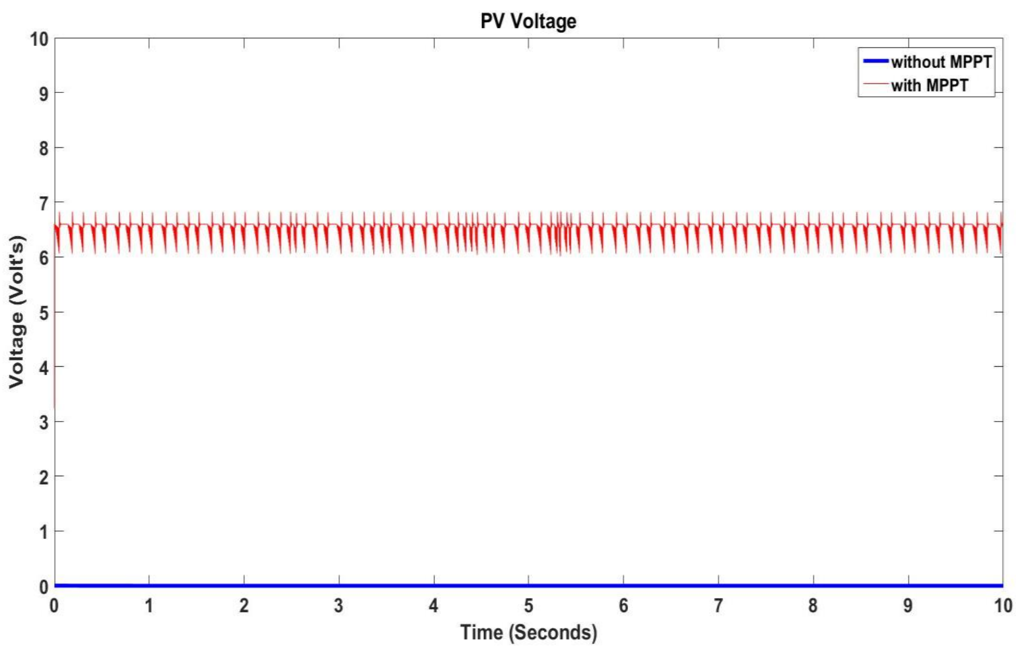

Fig. 1.27 shows the panel voltage with and without the controller and it is clear that the input voltage to the first stage is kept constant and at a value corresponding to MPP.

Above results justify the use of MPPT and charge controller as the additional circuit components as they are helping in achieving the objectives laid out in section 1.

Performance of the Scap (Supercapacitor) Charge Controller

Fig. 1.28 PV Input Power (Excess)

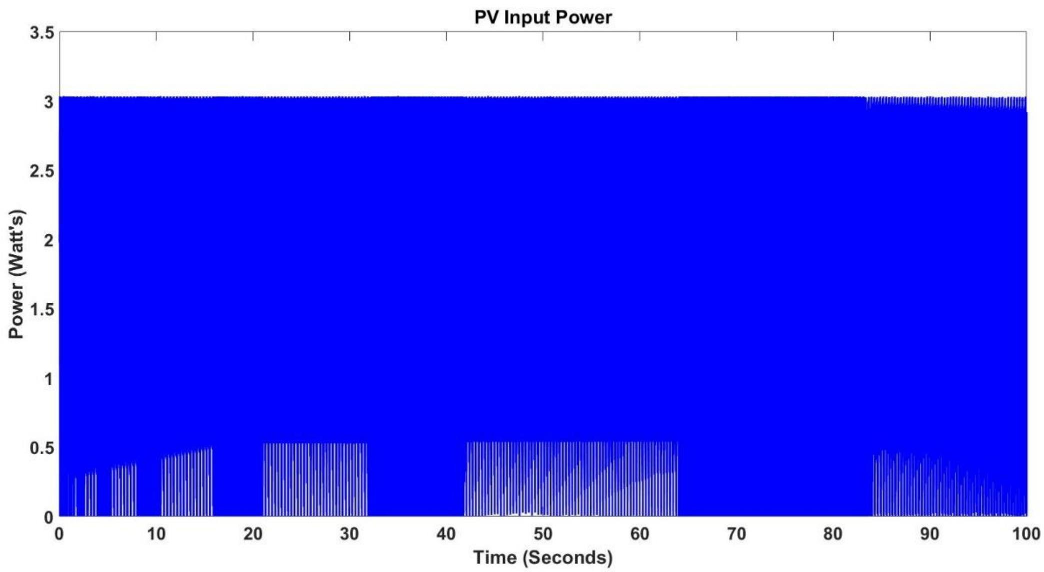

Fig. 1.29 Load Voltage Comparison (Excess)

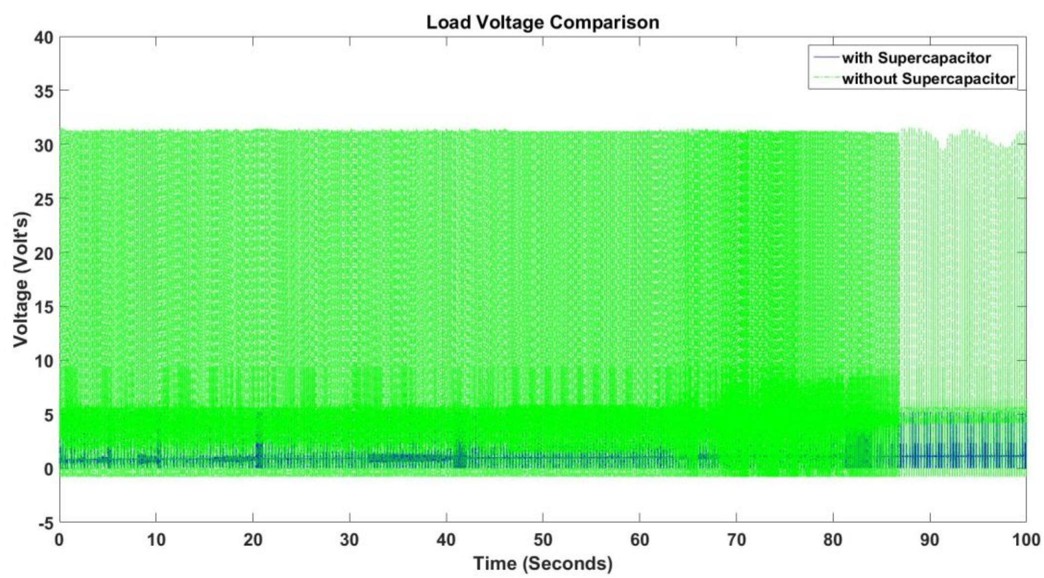

Fig. 1.28 shows the panel output power while operating at MPP (G = 800 W/m2). This condition corresponds to the excess power on DC which will result in overvoltage across the load (fig. 1.29 and 1.30).

Fig. 1.30 Load Voltage (Excess Power Mode)

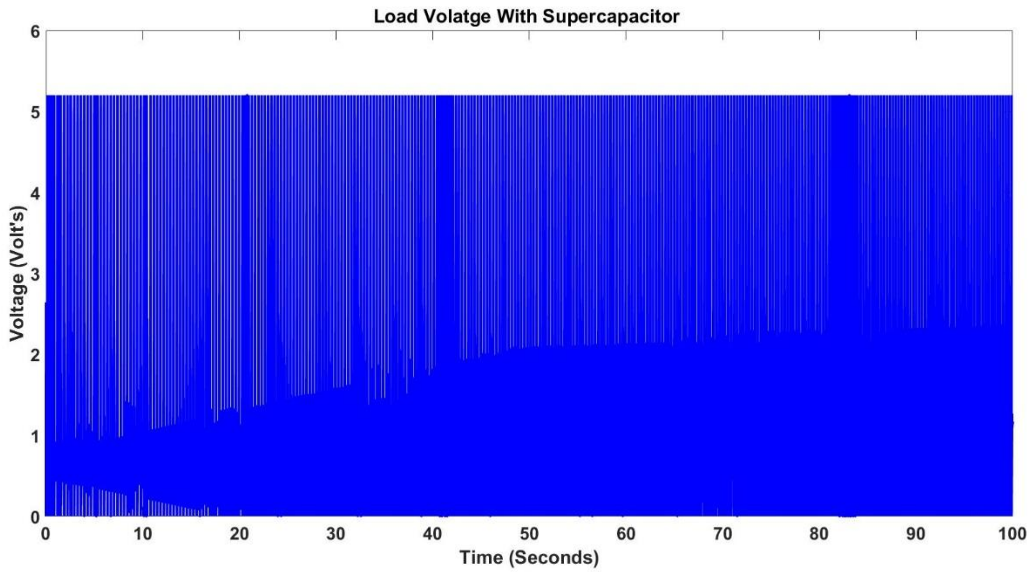

Fig. 1.29 and 1.30 clearly depict the overvoltage conditions existing when supercapacitor is not present and the panel is operating at MPP, it also shows the effect of adding supercapacitor to the circuit as the load voltage is reduced to 5 Volt's (Blue) which is the desired voltage profile at load terminals.

The following figures present a comparison of the battery charging current and the simulation results clearly indicate that with supercapacitor in the circuit the required battery charging profile (constant current) is maintained.

Fig. 1.31, Presents the battery charging current with supercapacitor

Fig. 1.32, Presents the battery charging current without supercapacitor

Fig. 1.31 Battery Charging Current (Excess Power Mode)

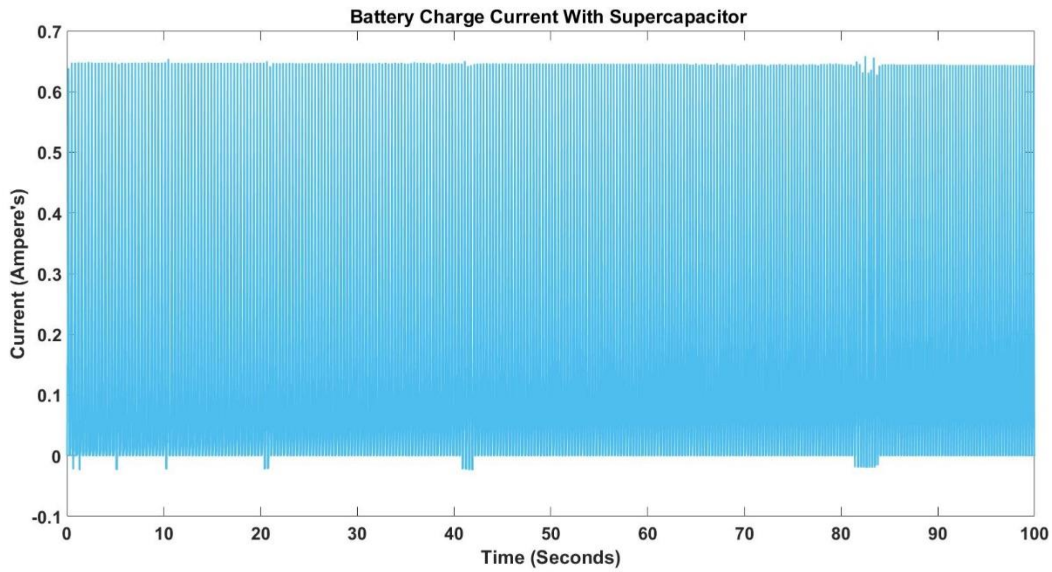

Fig. 1.32 Battery Charging Current (Excess Power Mode)

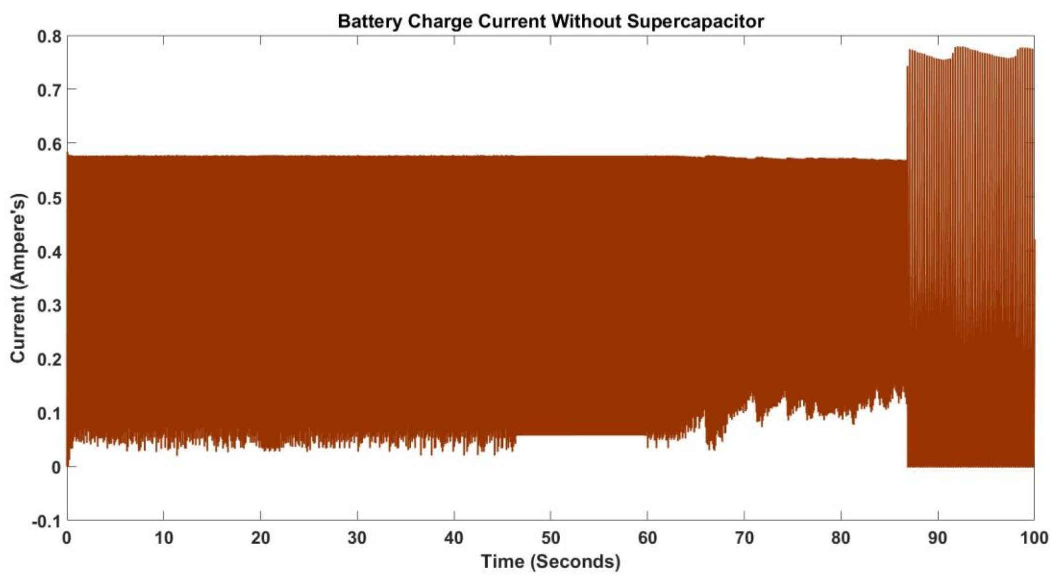

The purpose of supercapacitor in the circuit is to smoothen out the energy fluctuations, a condition which is normal when primary energy source (PV Panel) is intermittent in nature. Above results shows the effectiveness of the supercapacitor in case of excess power conditions.

Fig. 1.33 Supercapacitor Absorbing Excess Power

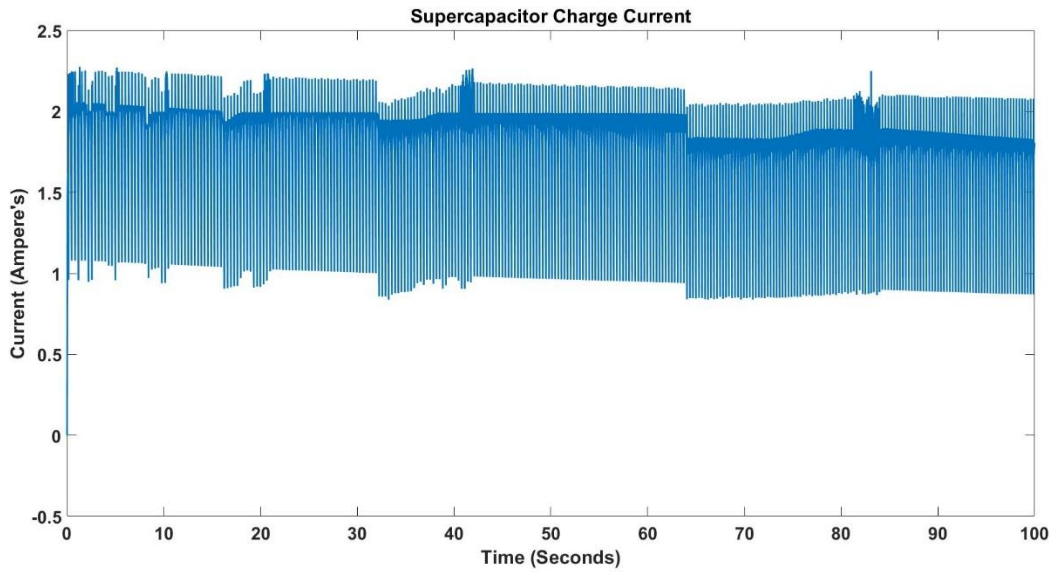

Above figure shows the value of supercapacitor current, it is varying in the range of 1 Amperes to 2.3 Amperes, as I_{MAX} rating for supercapacitor is 2.5 Amperes, this concludes that the performance of Scap charge controller is satisfactory.

Performance of the Scap (Supercapacitor) discharge controller

This controller is active whenever DC bus voltage falls below the desired value and supplements the panel in powering load and keep the desired profile for battery charging.

Power levels at different nodes during simulation are as follows: -

P_{IN} = 0.044 Watt's (fig.1.34)

P_{LOAD} = 0.025 Watt's (fig.1.35)

P_{BATT} = -1 Watt's (Battery is charging)

Fig. 1.34 PV Power (Deficit Power)

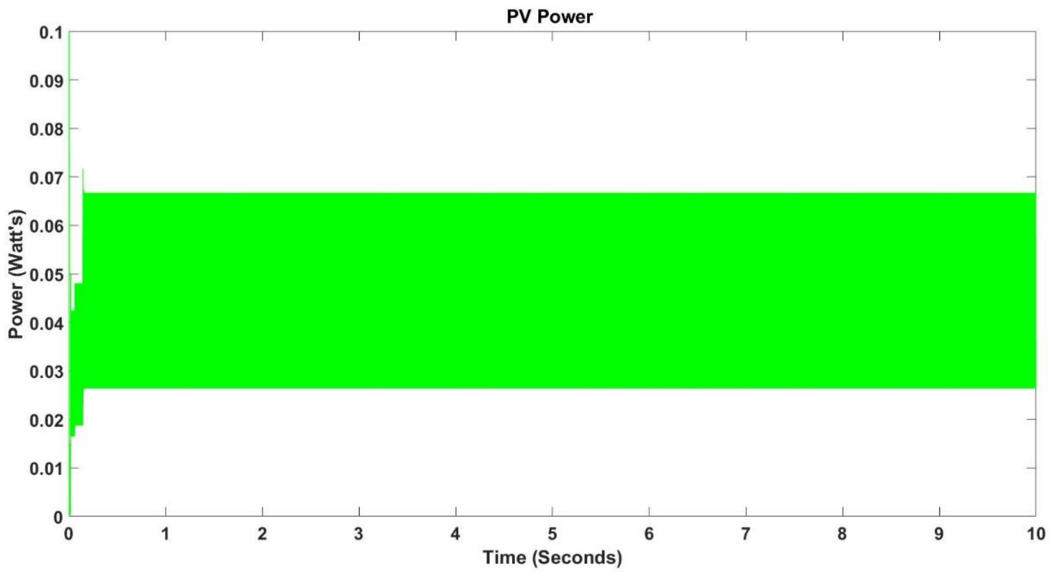

Fig. 1.35 Load Power

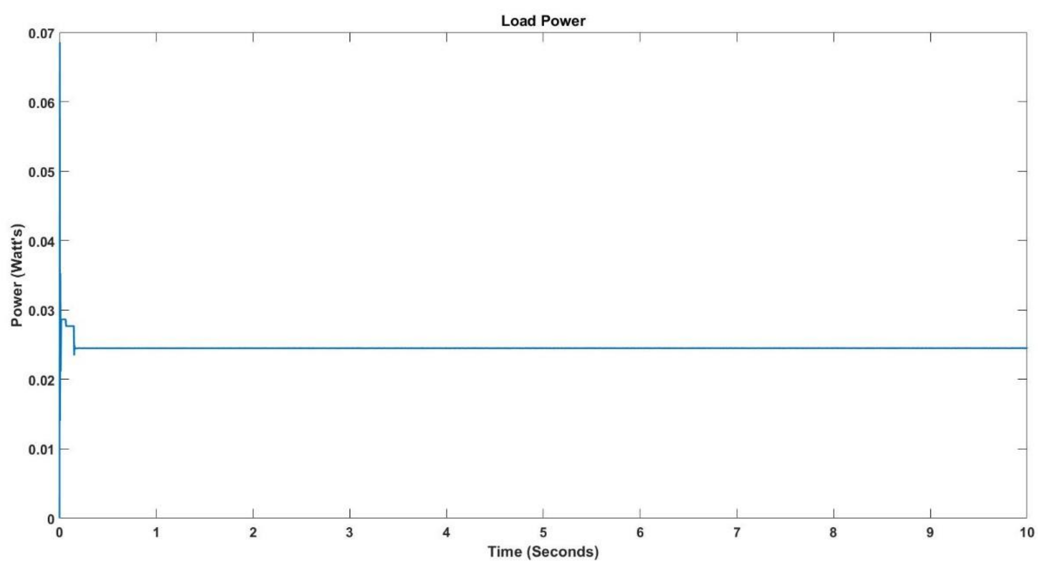

Fig. 1.36 Battery Charging Current (Deficit Mode)

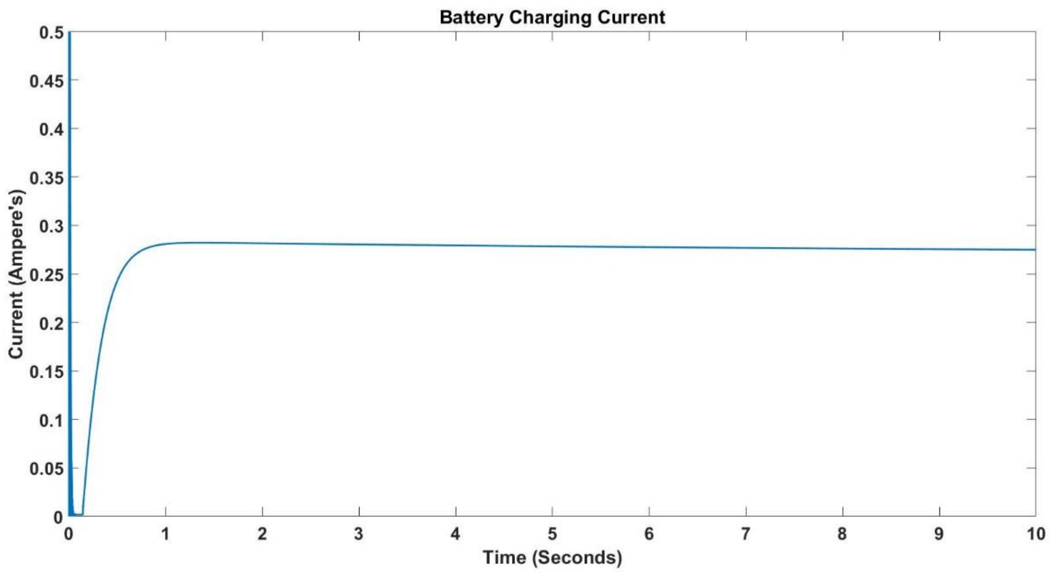

Fig. 1.37 Supercapacitor Power (Deficit Mode)

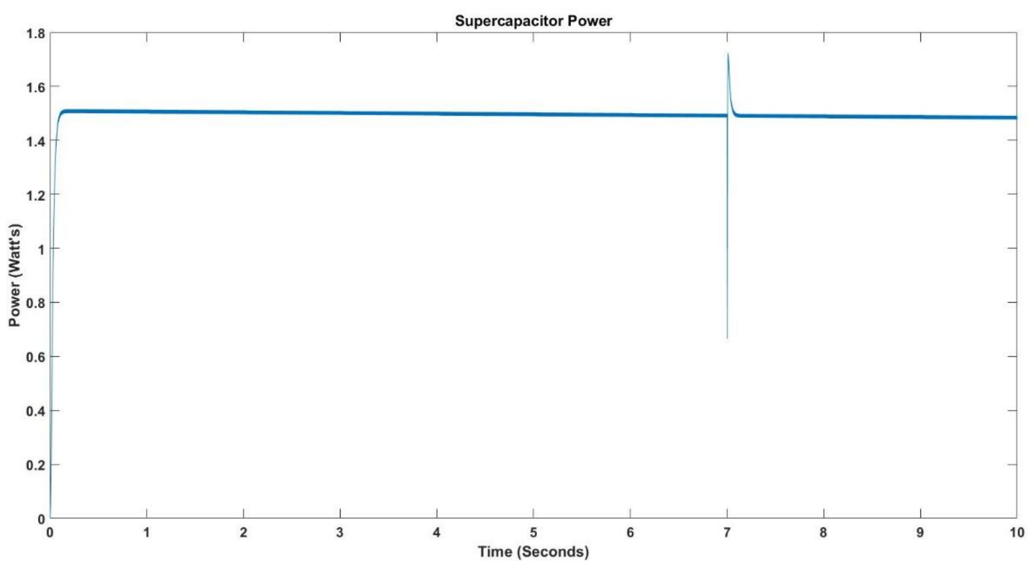

Fig.1.37 shows the power at supercapacitor terminals which are equal to the deficit power which is manifested by load voltage graph fig.1.38 (on next page).

Fig. 1.38 Load Voltage (Deficit Mode)

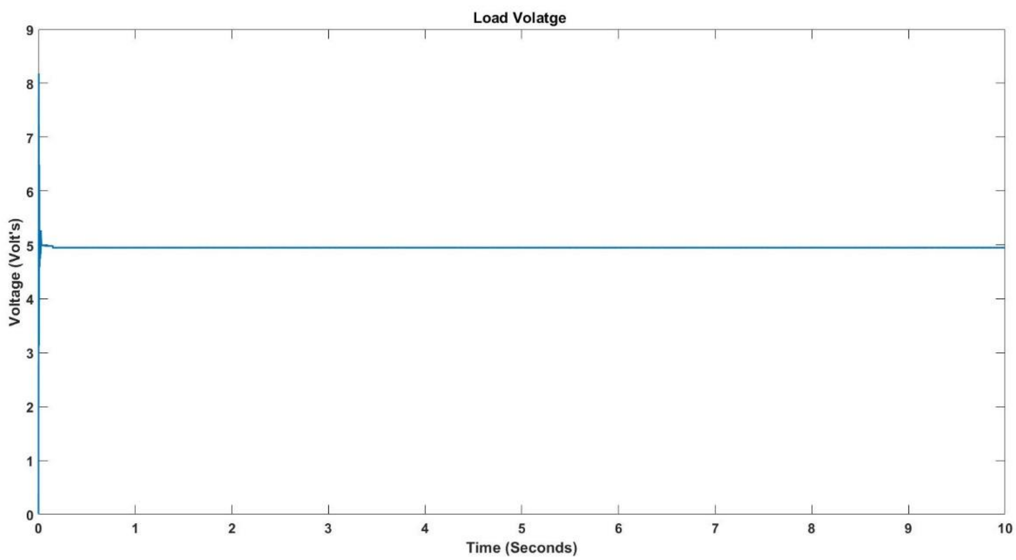

Fig. 1.39 Load Current (Deficit Mode)

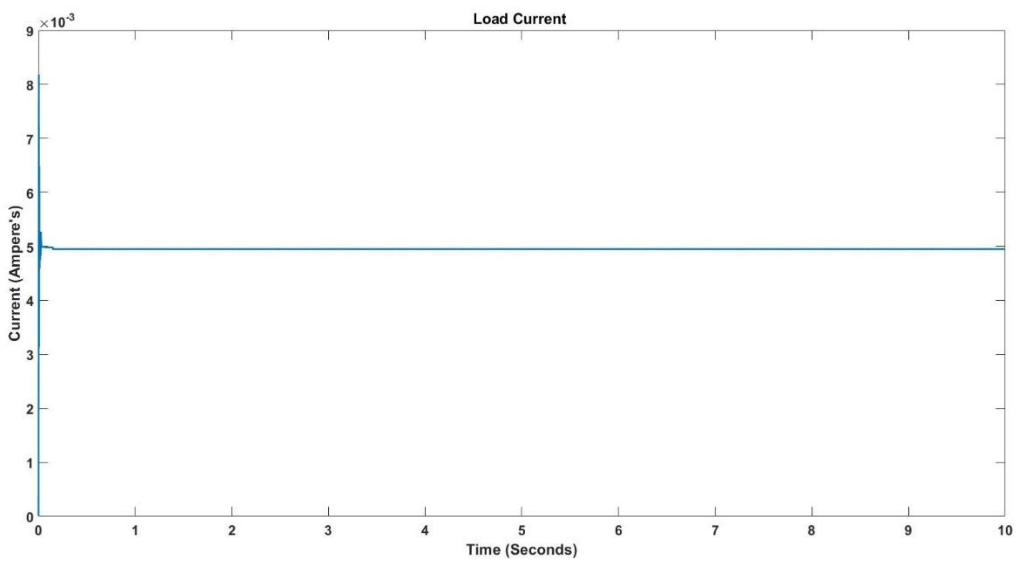

Fig. 1.38 and 1.39 confirm that the values of different variables are at desired level and hence it can be concluded that performance of Scap discharge controller is satisfactory.

The performance of the Battery Charge Scap Controller: -

Fig. 1.40 Battery Discharge Current (Night Mode)

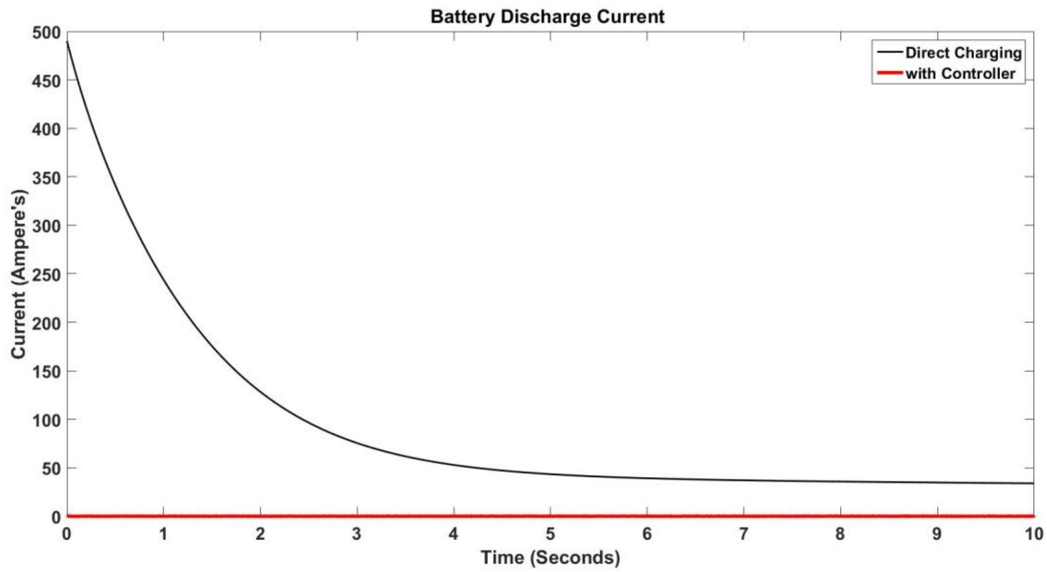

Fig. 1.41 Insite of Fig. 1.40

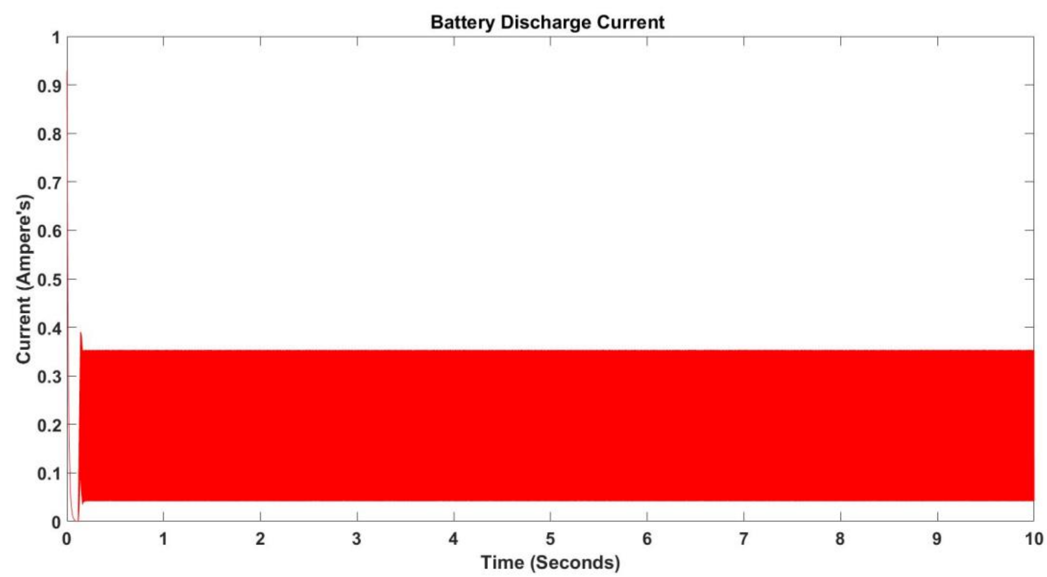

Fig. 1.40 compares battery discharge current while charging supercapacitor with and without the controller. This demonstrates the controller's ability to control the discharge as reduces the discharge current from 500 Ampere’s to 0.350 Ampere’s (fig.1.41).

Fig. 1.42 Battery Discharge Power (Night Mode)

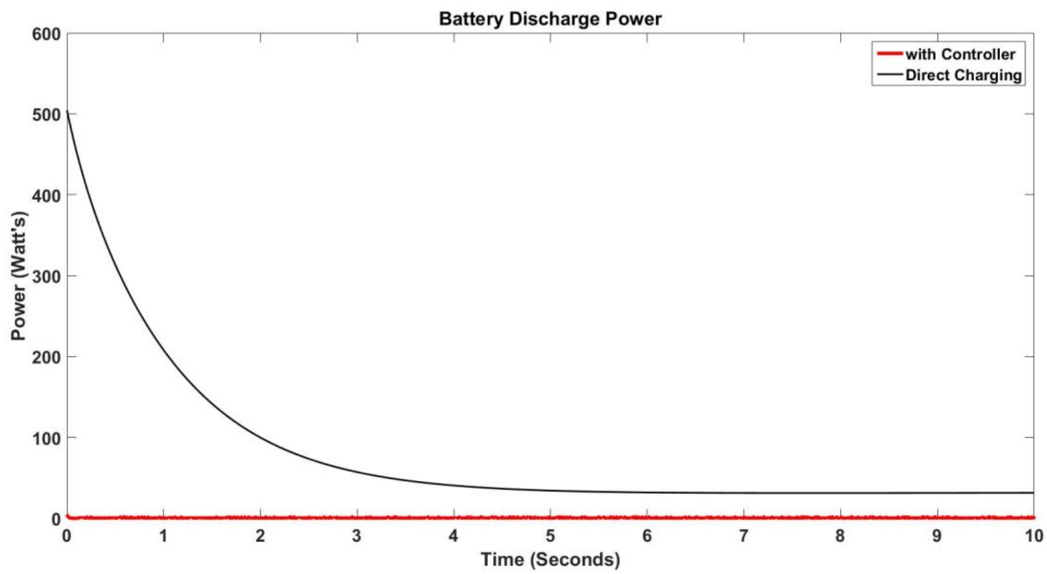

Above figure shows the power drawn with (Red) and without (Black) controller.

Fig. 1.43 Supercapacitor Charge Current (Night Mode)

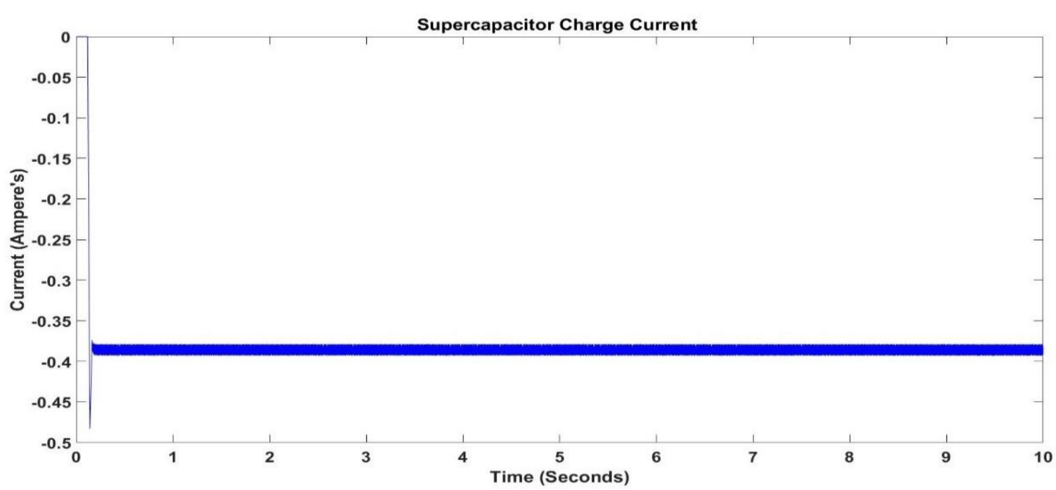

Fig. 1.44 Peak Load Current (Night Mode)

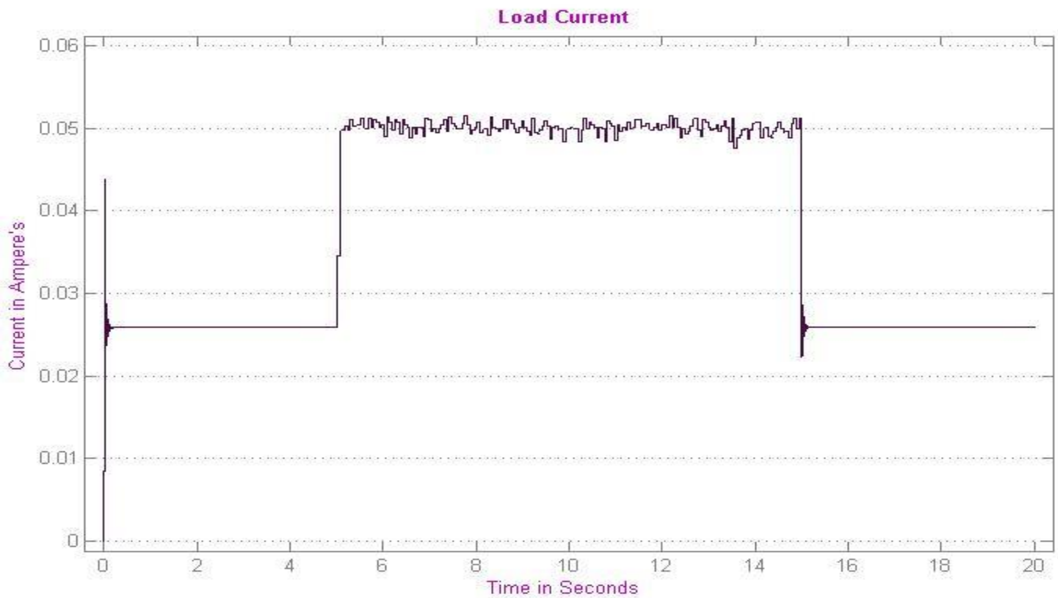

Fig. 1.45 Battery Discharge Current (Supplying Power to Scap)

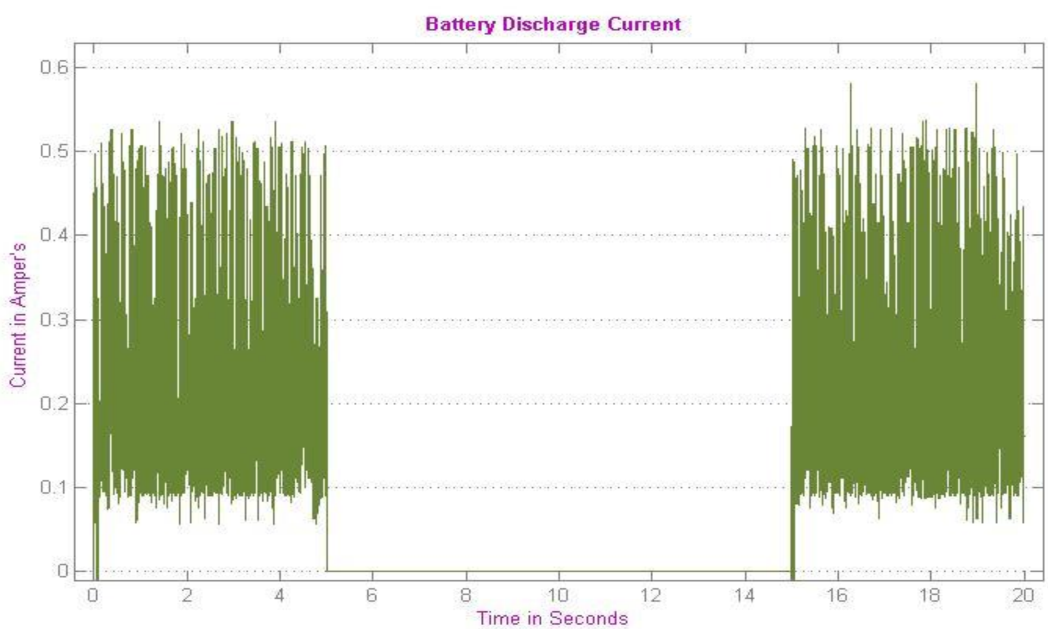

Fig. 1.46 Scap proving Peak Current (Night Mode)

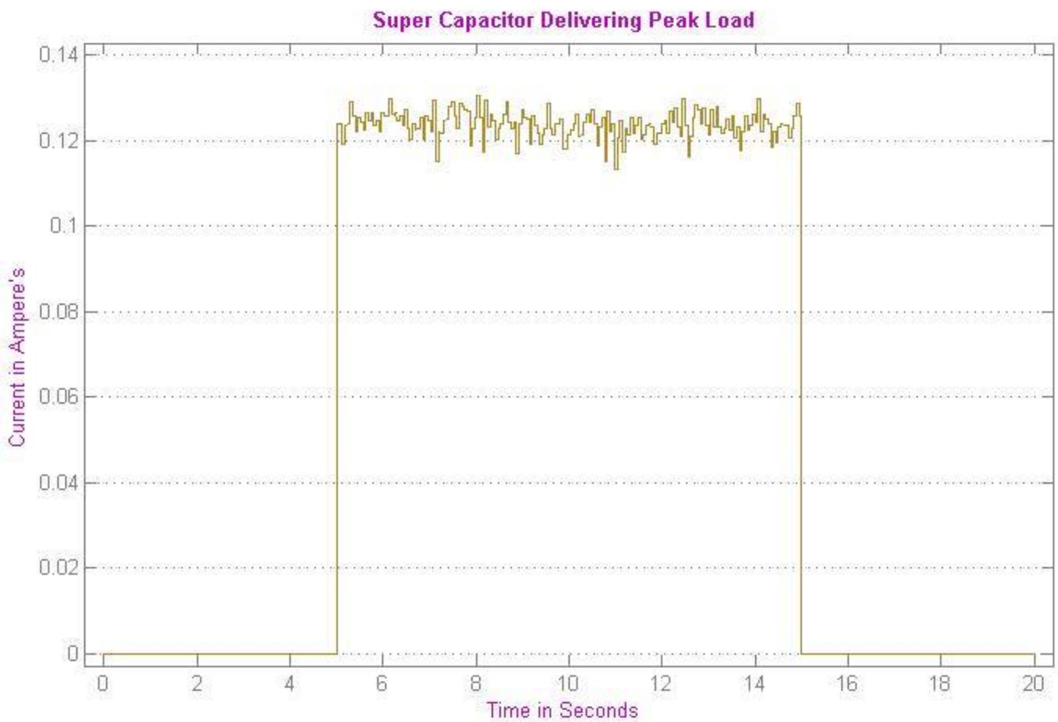

Fig. 1.44-1.46 shows the values of load, battery, and supercapacitor current values during the mode when P_{SOLAR} is not available and supercapacitor is charged from battery just before the arrival of peak power demand. The battery discharge current is 0.6 Ampere's which can be reduced to lower values by discharge controller as the duty of data sensing is very low in actual practice as compared to that which is carried out during simulation.

The simulation results presented in this section elucidate the role of different controllers in the circuit and provides an insight towards the different modes of operation of the circuit. These results also justifies the inclusion of additional circuitry like MPPT, Scap Controller etc.

Chapter 5

Hardware Implementation

5.1 Specification of the Components Used

PV Panel

Table 5.1

Parameter	Value
V_{OC}	11.6 Volt's
I_{SC}	0.61 Ampere's
R_S	0.1 Ohms
R_P	415.405 Ohms
V_{MP}	6.6 Volt's
I_{MP}	0.41 Ampere's
$P_{MAX.}$	5 Watt's

Supercapacitor

SAMWHA Green-cap (ELDC) having following characteristics [27] is used.

Table 5.2

Rated Voltage	2.7 Volts
Capacitance	400 Farad
ESR 1khz	3.0 milli Ohm
ESR DC	5.0 milli Ohm
LC (72 Hours)	1.08 mA
Max. Continuous Current Rating	22 Ampere's
Max. Peak Current	180 Ampere's
Specific Energy	5.79 Wh/Kg

Microcontroller

For implementing power manager and different controllers a c2000 f28027 Picolo Launchpad of Texas Instruments is used.

Fig. 1.47 LAUNCHXL-F28027 Board Overview [26]

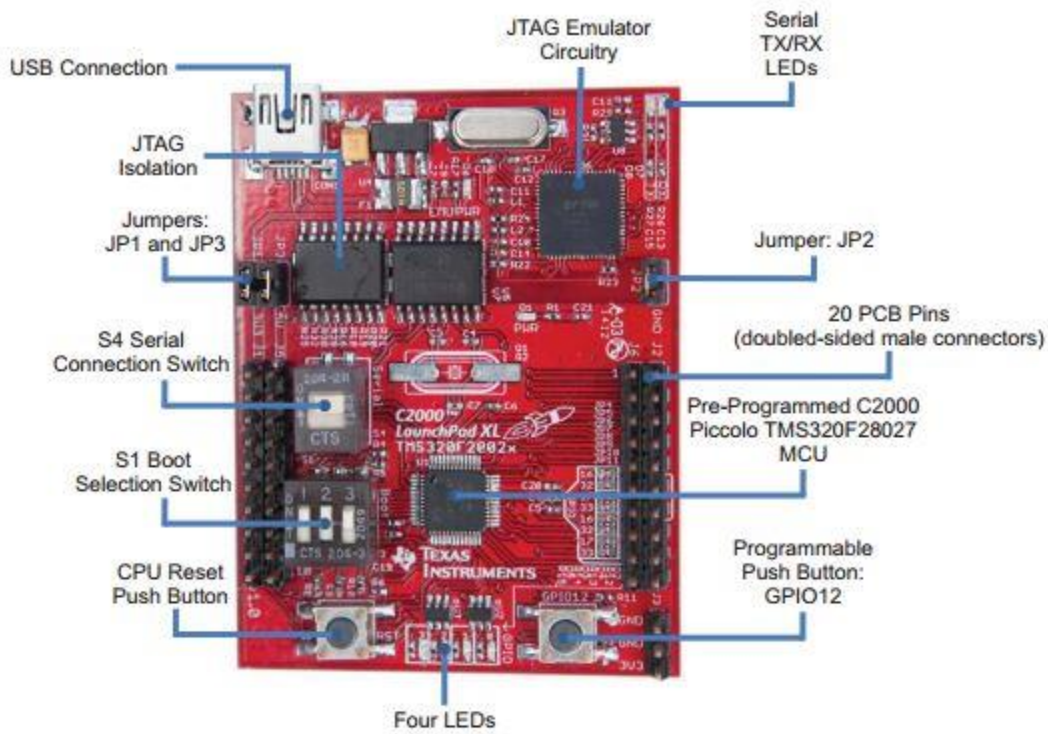

Table 5.3 [27]

Processor	TMS320F28027 32-bit
Operating frequency	60 MHz
Memory	32K Flash
RAM	6K
HRPWM Channels	4

Arduino Uno is used as the sensor node.

Battery

A Li-ion battery of capacity 700 miliamp_hours is used.

Sensor

A DHT 11 digital temperature and humidity sensor are used.

5.2 Programing c2000 microcontroller from Simulink MATLAB

The reason for choosing c2000 microcontroller for implementing different controllers is that it can be programmed directly from MATLAB using hardware support package.

Prerequisite

- ✓ A licensed MATLAB with RTW embedded coder.
- ✓ C28X Header Files and Peripheral Examples.
- ✓ Control Suite.
- ✓ CCS Version 6.1 or above.

<u>Procedure of programming c2000 from MATLAB</u>

MATLAB version 2015b

Step 1: - In Add-ons go to get hardware support package

Install from internet >> Texas Instruments c2000 >> Log in to Mathworks Account >> Accept License agreement >> download support package >> give the installation folder for header files >> give the installation folder for control suite

Step 2: - Setting up hardware for installed Support Package

On the command window type target updater and setup the compiler

Target updater >> embedded coder >> ccs 6.1

Step 3: - Setting up Model Configuration Settings in Simulink

Model configuration settings >> hardware implementation >> hardware board f28027 >> code generation >> ccs toolchain 6.1

Also check the solver settings as: -

Solver options

Type fixed step and solver discrete (with no continuous states)

Step 3: - Generating Code

Build your programming model using Simulink blocks and generate the code by using the control+b command.

For real-time implementation use Build, Load and Run in the code generation.

5.3 Programing model of MPPT for implementation on c2000 board

This MPPT model is run in a current loop which is hardware triggered, this interrupt is generated by end of ADC conversion. In the current loop, the ADC conversion is synchronized with ePWM output and the start conversion is triggered at the end of the period. The reason for this synchronization is to reduce the time lag in the control. For the faster execution of the current loop, it is run in the code_ramfuncs memory section. The model is shown below (fig.5.2, 5.3). The block having violet colored solid boundaries is the current loop.

Fig. 1.48 P and O

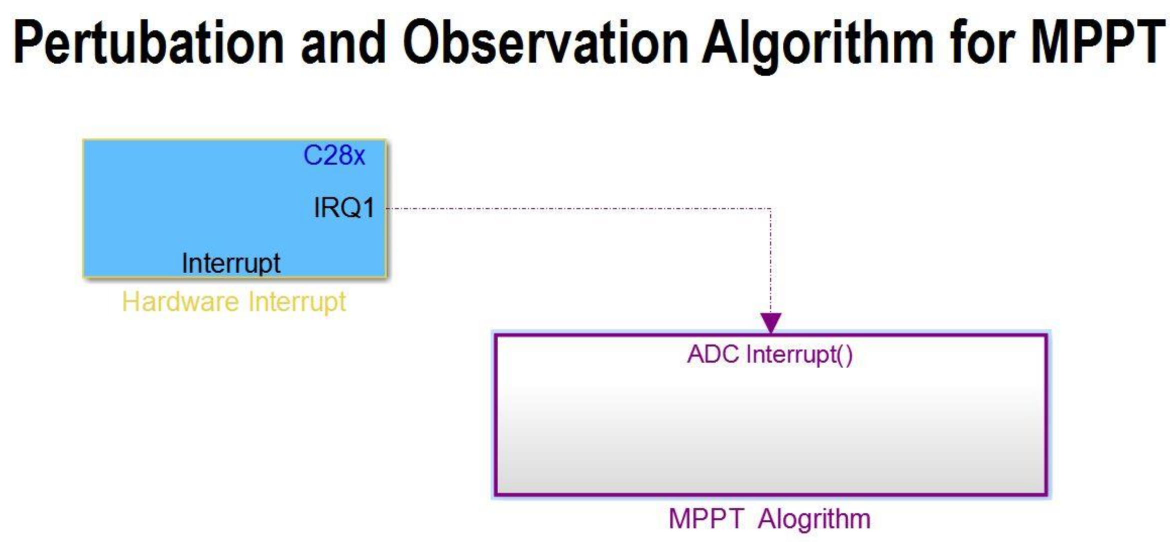

Fig. 1.49 Insite of P and O

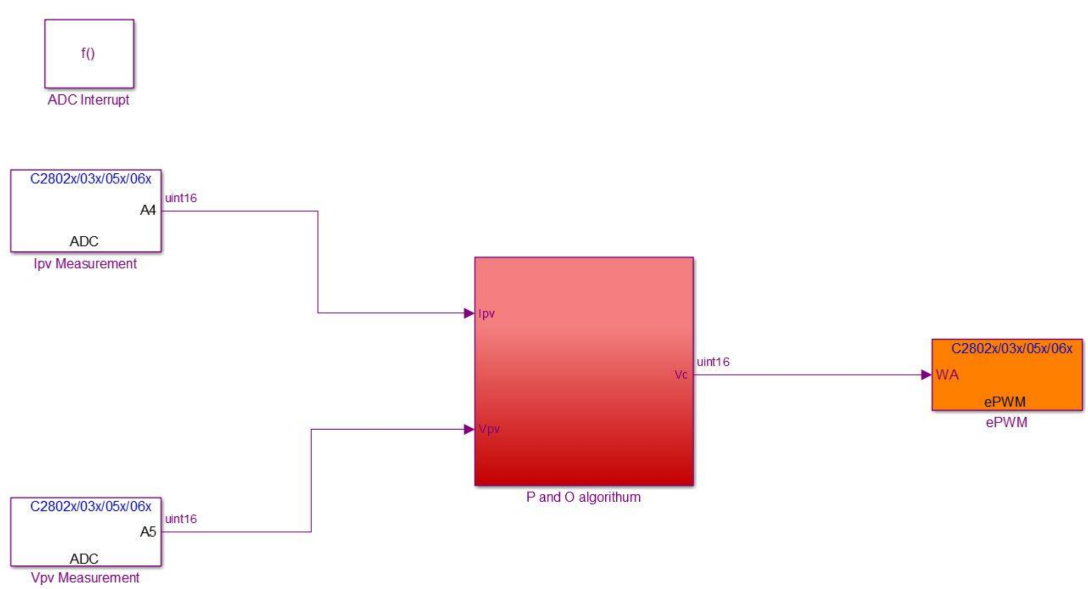

5.4 Programing Model of Battery Controller for implementation on c2000 board

As the battery controller is also taking analog input so it also requires a loop which is interrupt triggered and helps to synchronize the control with ADC conversion. Therefore, like MPPT control, the logic for battery control is also placed in the current loop and ADC start of conversion is synchronized with output PWM pulses. A rate transition block is placed in between the logic and ADC conversion block, this is done to stabilize the output.

Fig. 1.50 Battery Charge/Discharge Controller

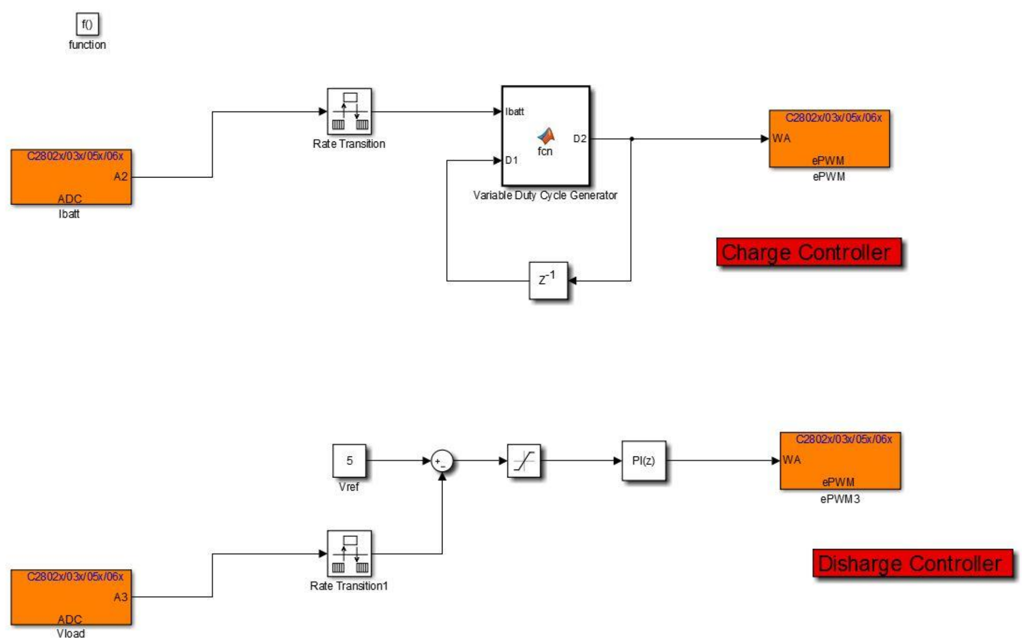

5.5 Programming model of Supercapacitor controller for implementation on c2000 board

The programming model of the supercapacitor is same as that of battery controller as both are using a PI controller in the closed loop control.

Fig. 1.51 Supercapacitor Charge/Discharge Controller

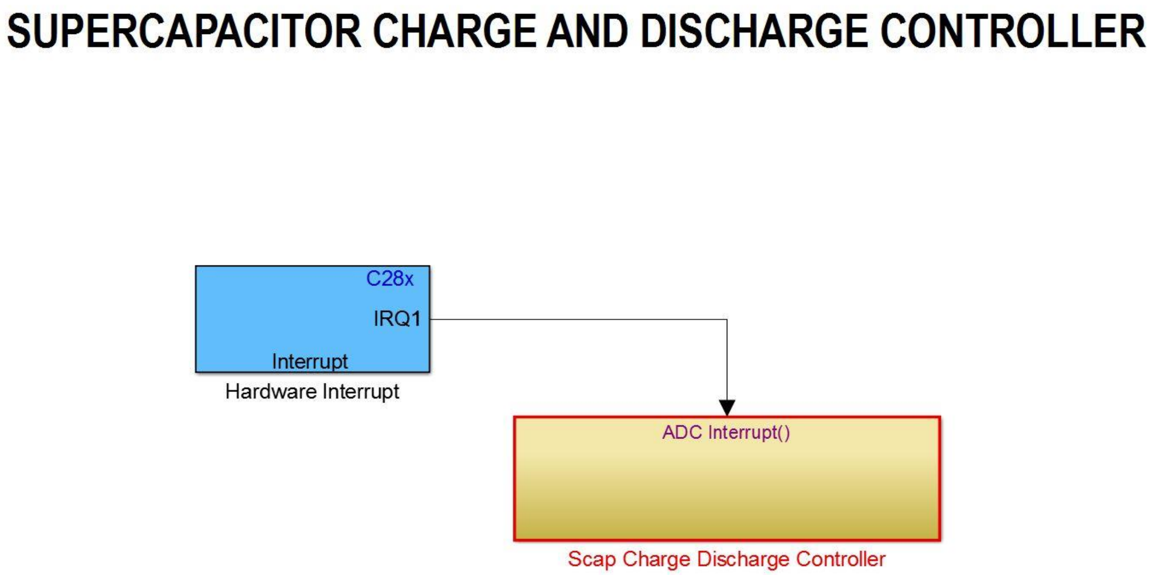

Fig. 1.52 Insite of fig.5.5

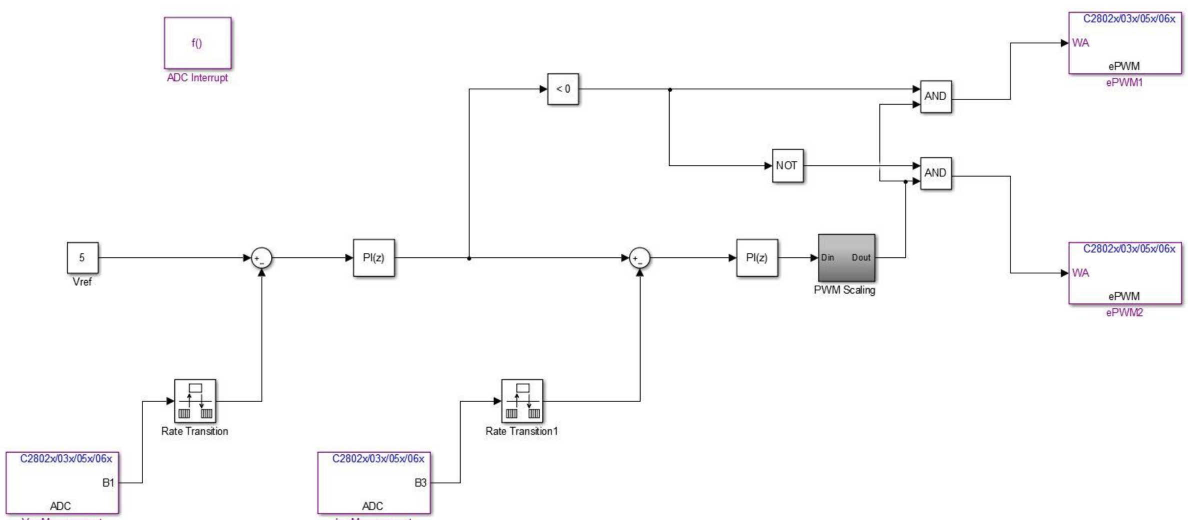

Chapter 6

Conclusions

In this work, a battery-supercapacitor hybrid storage technique is tested for solar powered WSN's to enhance the lifetime of the sensor node and to increase the computational power of the sensor node. The simulation results show that the battery discharge current is reduced to very low levels by software control and supercapacitor is dripped charged from it just before the arrival of peak power (Data Sensing, Data transmitting), this ensure that the discharge rate of the battery is low which will result in increased lifetime of the battery. By using the supercapacitor for supplying only peak power will reduce the auto consumption of

Scap converter and will improve the efficiency of the overall circuit. The problem of supercapacitor draining the battery (when P_{solar} is not available) will also be solved by using supercapacitor for supplying peak power only, as supercapacitor will be connected to internal DC bus only for short duration.

Generally, there is a tradeoff between computational power and node life-time. The reason being the dependence of cycle life of the battery on the discharge rate. In this design, no such tradeoff is required as supercapacitor (which is used to supply the peak power) has no such dependence on discharge rates.

The role of supercapacitor as energy buffer (when P_{solar} is available) is also tested as the simulation results show that battery charging current is maintained at a constant value under both excess and deficit power conditions on DC bus. This will further increase the cycle life of the battery as a constant charging profile is maintained.

The control logic used in Simulations is implemented on the c2000 Picolo Launchpad by using hardware support and embedded code. This will give a great flexibility and ease in programming as the board can be programmed directly from the MATLAB.

Recommendations

The following recommendations are suggested for extension of this work: -

- A PCB should be used for hardware implementation of the above circuit as bread board is inefficient especially for low power circuits.
- The protection scheme is necessary as the components used in the circuit are susceptible to overvoltage conditions which will occur in the circuit during transients.
- In the case of mismatch in simulation and hardware results, it is recommended that the PI controller is manually tuned by connecting the microcontroller to hardware circuit board.
- The possible reason for the mismatch in simulation and hardware results is the difference in behavior of the components physically as compared to the mathematical model used in simulations.
- The final stage for this will have to be done at the chip level and an I.C should be developed with effective choice of circuit components for efficient performance.

References

1. Randall, J. F., & Jacot, J. (2002). The performance and modeling of 8 photovoltaic materials under variable light intensity and spectra. In World Renewable Energy Congress VII & Expo (No. LPM-CONF-2002-006).
2. Choi, S. S., & Lim, H. S. (2002). Factors that affect cycle-life and possible degradation mechanisms of a Li-ion cell based on LiCoO 2. Journal of Power Sources, 111(1), 130-136.
3. Vullers, R. J., Van Schaijk, R., Visser, H. J., Penders, J., & Van Hoof, C. (2010). Energy harvesting for autonomous wireless sensor networks. IEEE Solid-State Circuits Magazine, 2(2), 29-38.
4. Raghunathan, V., Kansal, A., Hsu, J., Friedman, J., & Srivastava, M. (2005, April). Design considerations for solar energy harvesting wireless embedded systems. In Proceedings of the 4th international symposium on Information processing in sensor networks (p. 64). IEEE Press.
5. Li, Yin, and Ronghua Shi. "An intelligent solar energy-harvesting system for wireless sensor networks." EURASIP Journal on Wireless Communications and Networking 2015.1 (2015): 179.
6. Boicea, V. A. (2014). Energy storage technologies: The past and the present. Proceedings of the IEEE, 102(11), 1777-1794.
7. Jiang, X., Polastre, J., & Culler, D. (2005, April). Perpetual environmentally powered sensor networks. In Proceedings of the 4th international symposium on Information processing in sensor networks (p. 65). IEEE Press.
8. Pukhrem, S. (2013). A photovoltaic panel model in MATLAB/SIMULINK. Faculty of Electrical Engineering, Wroclaw University of Technology. Disponible en: https://www. research gate. net/publication/255721161_A_PHOTOVOLTAIC_PAN EL_MODEL_IN_MATLABSIMULINK.
9. Akhtar, F., & Rehmani, M. H. (2015). Energy replenishment using renewable and traditional energy resources for sustainable wireless sensor networks: A review. Renewable and Sustainable Energy Reviews, 45, 769-784.
10. Ongaro, F., Saggini, S., & Mattavelli, P. (2012). Li-ion battery-supercapacitor hybrid storage system for a long lifetime, photovoltaic-based wireless sensor network. IEEE Transactions on Power Electronics, 27(9), 3944-3952.
11. Sumathi, S., Kumar, L. A., & Surekha, P. (2015). Application of MATLAB/SIMULINK in Solar PV Systems. In Solar PV and Wind Energy Conversion Systems (pp. 59-143). Springer International Publishing.
12. Sumathi, S., Kumar, L. A., & Surekha, P. (2015). Solar PV and wind energy conversion systems: an introduction to theory, modeling with MATLAB/SIMULINK, and the role of soft computing techniques. Springer.
13. Hande, A., Polk, T., Walker, W., & Bhatia, D. (2007). Indoor solar energy harvesting for sensor network router nodes. Microprocessors and Microsystems, 31(6), 420-432.
14. Minami, M., Morito, T., & Morikawa, H. (2005). Biscuit: A battery-less wireless sensor network system for environmental monitoring applications. In In Proc. of the 2nd International Workshop on Networked Sensing Systems.

15. Jiang, X., Polastre, J., & Culler, D. (2005, April). Perpetual environmentally powered sensor networks. In Proceedings of the 4th international symposium on Information processing in sensor networks (p. 65). IEEE Press.
16. Li, W., Zheng, Y., Li, W., & He, X. (2010, February). A smart and simple PV charger for portable applications. In Applied Power Electronics Conference and Exposition (APEC), 2010 Twenty-Fifth Annual IEEE (pp. 2080-2084). IEEE.
17. Naveen, K. V., & Manjunath, S. S. (2011, September). A reliable ultracapacitor based solar energy harvesting system for wireless sensor network enabled intelligent buildings. In Intelligent Agent and Multi-Agent Systems (IAMA), 2011 2nd International Conference on (pp. 20-25). IEEE.
18. Basic Calculation of a Buck Converter's Power Stage. Application Report SLVA477B–December 2011–Revised August 2015
19. Basic Calculation of a Boost Converter's Power Stage. Application Report SLVA372C–November 2009–Revised January 2014
20. Walker, G. (2001). Evaluating MPPT converter topologies using a MATLAB PV model. Journal of Electrical & Electronics Engineering, Australia, 21(1), 49.
21. Lorenzo, E. (Ed.). (1994). Solar electricity: engineering of photovoltaic systems. Earthscan/James & James.
22. González-Longatt, F. M. (2005). Model of photovoltaic module in Matlab. Ii Cibelec, 2005, 1-5.
23. González-Longatt, F. M. (2005). Model of photovoltaic module in Matlab. Ii Cibelec, 2005, 1-5.
24. Ramos-Hernanz, J. A., Campayo, J. J., Larranaga, J., Zulueta, E., Barambones, O., Motrico, J., ... & Zamora, I. (2012). Two photovoltaic cell simulation models in Matlab/Simulink. International Journal on Technical and Physical Problems of Engineering (IJTPE), 4(1), 45-51.
25. Sumathi, S., Kumar, L. A., & Surekha, P. (2015). Application of MATLAB/SIMULINK in Solar PV Systems. In Solar PV and Wind Energy Conversion Systems (pp. 59-143). Springer International Publishing.
26. LAUNCHXL-F28027 C2000 Piccolo LaunchPad Experimenter Kit. SPRUHH2A. January 2014
27. Green-Cap (ELECTRIC DOUBLE LAYER CAPACITORS).
28. Lin, K., Yu, J., Hsu, J., Zahedi, S., Lee, D., Friedman, J., ... & Srivastava, M. (2005, November). Heliomote: enabling long-lived sensor networks through solar energy harvesting. In Proceedings of the 3rd international conference on Embedded networked sensor systems (pp. 309-309). ACM.
29. Raghunathan, V., Kansal, A., Hsu, J., Friedman, J., & Srivastava, M. (2005, April). Design considerations for solar energy harvesting wireless embedded systems. In Proceedings of the 4th international symposium on Information processing in sensor networks (p. 64). IEEE Press.
30. Walker, G. R. (2000). Evaluating MPPT converter topologies using a MATLAB PV model. AUPEC 2000: Innovation for Secure Power, 1, 138-143.
31. MICA2DOT WIRELESS MICROSENSOR MOTE. 6020-0043-03. 2007
32. Lorenzo, E. (Ed.). (1994). Solar electricity: engineering of photovoltaic systems. Earthscan/James & James.